Crystallization of one Protein from a Raw Material

-case study of L-asparaginase II from *Escherichia coli* cells-

Dissertation

Zur Erlangung des

Doktogrades der Ingenieurwissenschaftern (Dr.-Ing.)

des Zentrums für Ingenieurwissenschaften

der Matin-Luther-Universtät

Halle-Wittenberg

vorgelegt

von Frau M. Sc. Yi Liu

geb. am 21.09.1983 in Zhejiang, China

Gutachter: 1. Prof. Dr.-Ing. habil. Dr. h.c. Joachim Ulrich

2. Prof. Dr. rer. nat. habil. Markus Pietzsch

3. Prof. Izumi Hirasawa

Datum der Verteidigung: 21.05.2014

Acknowledgements

Table of Contents

1. Introduction

Crystallization is known as a procedure of thermal separation which requires a thermodynamic non-equilibrium condition as a driving force to induce the nucleation and the following crystals growth. Since the first successful crystallization of hemoglobin from the earthworm by Hünefeld in 1840 [Mc99], protein crystallization has served as a critical scientific tool to purify one protein from another. The fact that the Nobel Prize for Chemistry was awarded for the outstanding work of Summer, Nothrop, and Stanley in the application of protein crystallization in purification and classification of biological chemicals in 1946 [Wie02] shows the importance of crystallization in protein separation. Especially, with the advent of the recombinant DNA technology, there is a large demand for many proteins to be purified by crystallization for the pharmaceutical utilization [Wie02] [Mar08] [Ger08].

In the present work, L-asparaginase II was chosen as the case study due to its effective inhibition of acute lymphatic leukemia (ALL) in patients reported by Rauenbusch et al. [Rau70]. Since 1967, many scientists have been making to develop a technical process for the production of L-asparaginase II as an enzyme. In the early studies, scientists, such as Robert et al. [Rob68], Rauenbusch et al. [Rau70], Ho et al. [Ho69][Ho70] and Wagner et al. [Wag71] [Wag73], had developed the procedures for the purification of L-asparaginase II by precipitation steps followed by crystallization. However, little attention was paid on the mechanism of crystallization behavior of L-asparaginase II in solution.

Theoretically, in order to well control the optimal supersaturation level in a crystallizer, a phase diagram including a metastable zone width (MZW) is crucial [Hof13]. Compared with the conventional molecules, there remain many surprising difficulties in protein crystallization, what might stem from the complicated structure of proteins and enzymes. To date, Lysozyme, the most common subject of protein crystallization studies, has possessed a set of established phase diagrams [Cac91][Pus88][Mus97][Ryu12][Ald09][Mül11b][Liu10][Mao12].

By contrast, the available data concerning crystalline L-asparaginase II, such as, solubility curves, nucleation curves and MZW, are limit. Even though the method of purifying L-asparaginase II based on the solution crystallization supplemented with a given precipitant agent had been investigated (as mentioned above), there are no

information of its crystallization behavior with respect to a solution system, especially, for a multi-component system.

For those reasons, the present work is focusing on the investigation of the crystallization behavior of L-asparaginase II by an online turbidity technique. In order to well understand the crystallization behavior of L-asparaginase II from a raw material, i.e., in a multi-component system, the commercial product was discarded. Instead, the protein of interest was fresh extracted from the recombinant *Escherichia coli cells*. The screening tests were performed by a simple method of crystallization in solution. The X-ray diffraction technique was also utilized to analyze the internal components of the protein crystals over the range of conditions studied. It hopes to provide useful information guiding the crystal growth of L-asparaginase II in a multi-component system, when the crystallization as a technique serves as a purification and separation method in industrial application.

2. STATE OF THE ART

2.1 Classical Theory of Crystallization

Compared with other chemical compounds, protein crystallization is regarded a new member who just joined in the family of crystallization in 1840 when hemoglobin from the earthworm was crystallized in slowly drying between two slides of glass by Hünefeld [Mc99]. To date, there is not a general principle to summarize the theory of protein crystallization. However, despite this theory deficiency, the classical theory for small molecule crystallization can be borrowed to understand the process of protein crystallization.

Actually, crystallization is a process of solid-liquid separation, which consists of two major kinetics, nucleation and crystal growth. A non-equilibrium condition is crucial in the system as a driving force for the process. The level of supersaturation in the case of solutions or melts could play the role of a driving force. In the case of solution, supersaturation level can be reached when the liquid phase is in contact with the solid phase, or saying in other words, the solute exceeds the solubility limit in a solution resulting in the formation of clusters [Ulr06]. The nucleation mentioned above is the mechanism of primary homogeneous nucleation. Other nucleation mechanisms are illustrated in Figure 2.1-1 [Mul01].
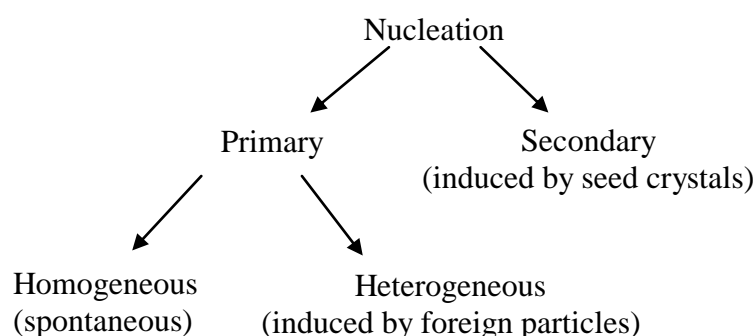
Figure 2.1-1: Scheme of nucleation [Mul01]

In either case, the difficulty of nuclei formation depends on the nucleation free energy barrier ΔG_{nuc} (as shown in Figure 2.1-2). Firstly the free energy of aggregates increases with size, and then it reaches a maximum when the aggregate size reaches

the critical nucleus size. Afterwards, the free energy decreases resulting in a rapid growth rate of nuclei to form ordered crystals.
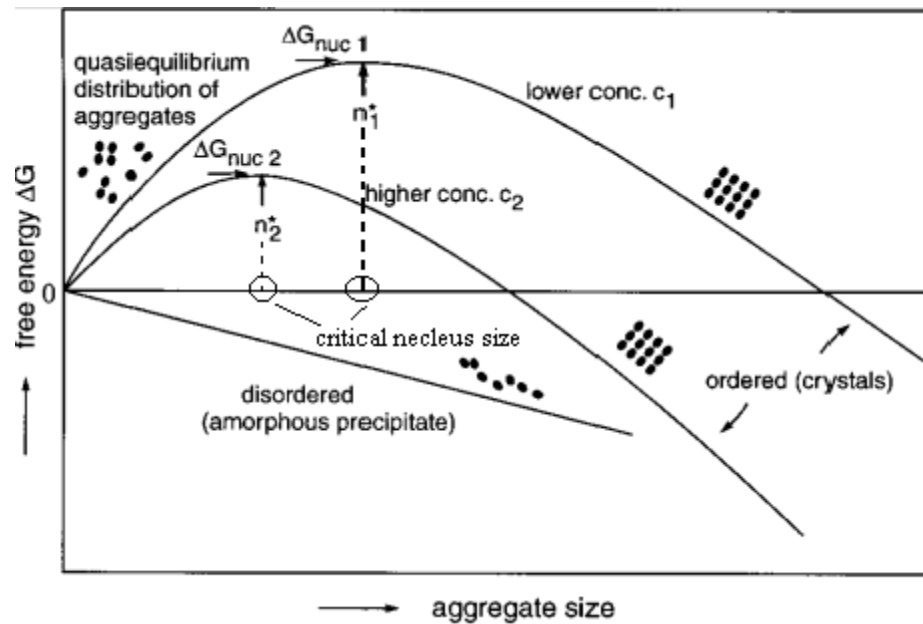
Figure 2.1-2: Free energy of aggregates as a function of aggregate size [Dur96]

In classical theory of crystallization, the nucleation rate in a given solvent could be expressed in the Equation 2.1-1 [Sch13]:

$$J = J_0 \exp\left(-C_s \frac{\gamma_n^3 V_{mol}^2}{k^3 T^3 (lnS)^2}\right) \tag{2.1-1}$$

J_0 is the pre-exponential factor, C_s is the geometry of the nucleus, γ_n is the interfacial energy of the nucleus in a given solvent, V_{mol} is the molecular volume, k is the Boltzmann constant (gas constant per molecule is 1.3805×10^{-23} J K^{-1}), T is the temperature and S is the relative supersaturation. From this equation it could be understood that the main three factors, temperature T, supersaturation degree S and interfacial energy γ, dominate the rate of nucleation. However, the surface energy could be neglected concerning small molecular aggregates of critical nucleus size [Mul01].

The rate of crystal growth depends on the temperature level, supercooling (driving force), fluid dynamics, and so on. Along with the kinetics, the thermodynamics (temperature and pressure concentration) of a system is also a factor to control any thermal separation process. Pressure is often constant in industrial crystallization

processes. Theoretically, the thermodynamics gives the operational window to produce crystals, while the kinetics decides the costs (time and the size of equipment) required for crystallization [Ulr06]. The two key points regarding a design of crystallizers are normally discussed separately. However, in practice, knowing the solubility limit of a crystallization process which is defined by thermodynamics is only one part. It is also important to know the finite time-scale conducted by kinetics, e.g., the nucleation line or in other words the metastable zone width [Ulr06]. Therefore, in the present work, the phase diagram contains both nucleation limit and the solubility curve.

Here, a phase diagram plotting protein concentration as a function of temperature (as shown in Figure 2.1-3) could be as an example to understand the mechanism in a real process of crystallization. Every solid has a unique solubility in a certain solvent at a given condition, which is illustrated as a solubility curve in Figure 2.1-3. A supersaturated level can be achieved when the solution is cooled until it reaches a temperature, at which the nuclei will form spontaneously due to the solute concentration in the solution exceeding the solubility limit (above the solubility curve) and very close to the nucleation curve (see Figure 2.1-3). As more nuclei form, the solute in the solution is consumed and the supersaturation level of the solution system will beyond the metastable limit and then entre the area between the metastable limit and solubility curve, which is the so called metastable zone. In this region, new nuclei are not able to form but the present nuclei will grow continuously until the equilibrium level of the solution (move back to the solubility curve) rebuilds [Ulr06].
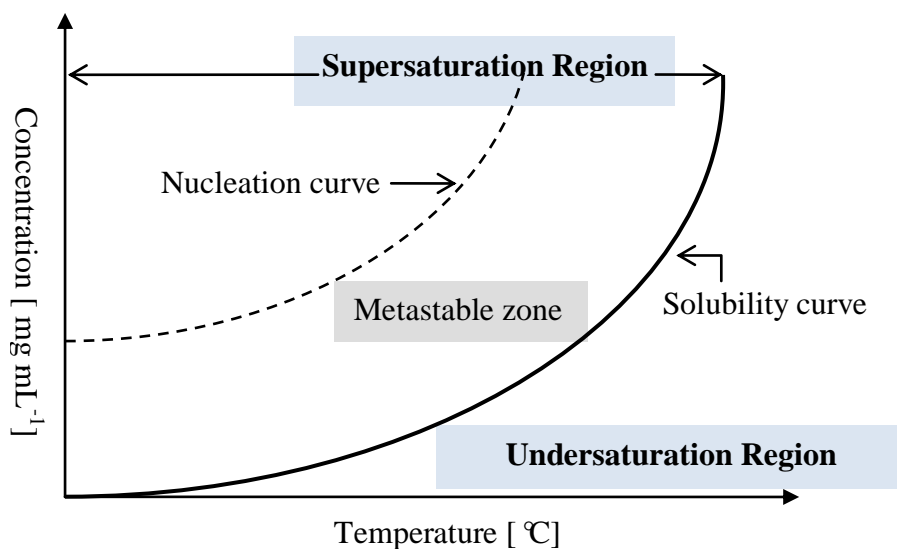
Figure 2.1-3: The phase diagram of crystallization in solution [Ulr06]

2.2 Proteins and Enzymes

In comparison with conventional small molecules, the process of macromolecular crystallization is more complicated and difficult due to their complexity of internal structure. Thus, proteins or enzymes are very sensitive with changes of the pH value, pressure, and solvents in the solution system [Mc09]. The protein-protein contacts become weaker with an increase of its molecular weight. Another factor arising as a problem in the process of protein crystallization is that the high demand of pure protein of interest is difficult to meet [Dur96][Mc99].

 Before carrying out the crystallization of the protein of interest, the nature of the structure of a protein must be understood. Proteins are macromolecules and are considered as polymers of amino acids arranged in a linear chain and folded into a globular form [Wie02].

Most proteins fold into unique 3D structures. Usually, a protein structure can be described into four levels [Wie02]:

Primary structure: The amino acid sequence

Secondary structure: Regular repeating local structures stabilized by hydrogen bonds, e.g. α-helix, β-sheet and turns.

Tertiary structure: The overall shape of a single protein molecule and the spatial relationship of the secondary structures to one another.

Quaternary structure: The structure formed by several protein molecules.

 The amino acids in a polymer chain are joined together by the peptide bonds between the carboxyl and amino groups of adjacent amino acid residues (shown in Figure 2.2-1). There are 20 amino acids found in natural proteins (as shown in Figure 2.2-2) [Wie02]. The natural proteins are built up by multiple amino acids (among those 20 amino acids mentioned above). Every two amino acids join together by losing one molecule of water.

$$^+H_3N — \underset{\underset{R}{|}}{\overset{\overset{COO^-}{|}}{C}} — H$$
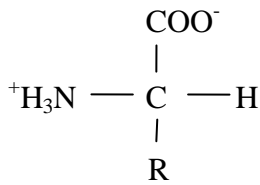
Figure 2.2-1: Chemical structure of the peptide bond [Wie02]. The R group is defined for the various amino acids

As shown in Figure 2.2-2, the side chains of amino acids comprising proteins are nonpolar, polar, basic and acidic, which add together to provide a protein with a net charge. Thus, protein is an amphoteric molecule which possesses a minimum solubility in water or salt solutions at the pH corresponding to their isoelectric point (pI), at which protein molecules carry no net charge and can be precipitated out of the solution [Wie02].

The molecular weight of a protein is typically expressed in terms of the unit kilodalton (kDa). Protein larger than 15kDa usually contains multiple domains. Domains are units of folded protein that may be linked by no more than a single polypeptide bridge, and often the units are both structurally and dynamically independent. Even a protein of a single domain exhibits flexibility that may cause motions into solvent and interaction with neighbors in solution [Mc99]. Thus, these complicated natures of protein with motions will provide influences during crystallization in the solution.

One of the important roles of proteins in the cell is an enzyme to catalyze chemical reactions. Most enzymes are proteins with globular shapes, and like all proteins, enzymes are long, linear chains of amino acids that fold to construct a 3D product. Each unique amino acid sequence produces a specific structure, which has unique properties. Different from other normal proteins, enzymes serve as catalysts and are usually highly specific and accelerate only one or a few chemical reactions [Enz13]. The reacting molecule that binds to the enzyme is called the substrate which is complementary in shape that of the active site. It was thought that the substrate exactly fitted into the active site of the enzyme molecule like a key fitting into a lock. This explains why an enzyme would only work on one substrate [Fis94]. However, this lock and key theory fails to explain the stabilization of the transition state that enzymes achieve. Therefore, Koshland [Kos58] suggested that the active site is continuously reshaped by interactions with the substrate as the substrate interacts with

the enzyme, that is to say, the amino acid side-chains which make up the active site are molded into the precise positions that enable the enzyme to perform its catalytic function (shown in Figure 2.2-3).

For this reason, the catalytic activity is an important value to estimate their presence and the specific activity (total activity divided by protein concentration) can show the purity of a protein [Mc99]. In accordance with international practices, an international unit, that is U, is applied to define that amount of enzyme which catalyzes the formation of 1 μmol of product per min at a given condition (e.g. pH, temperature) [Ho70].
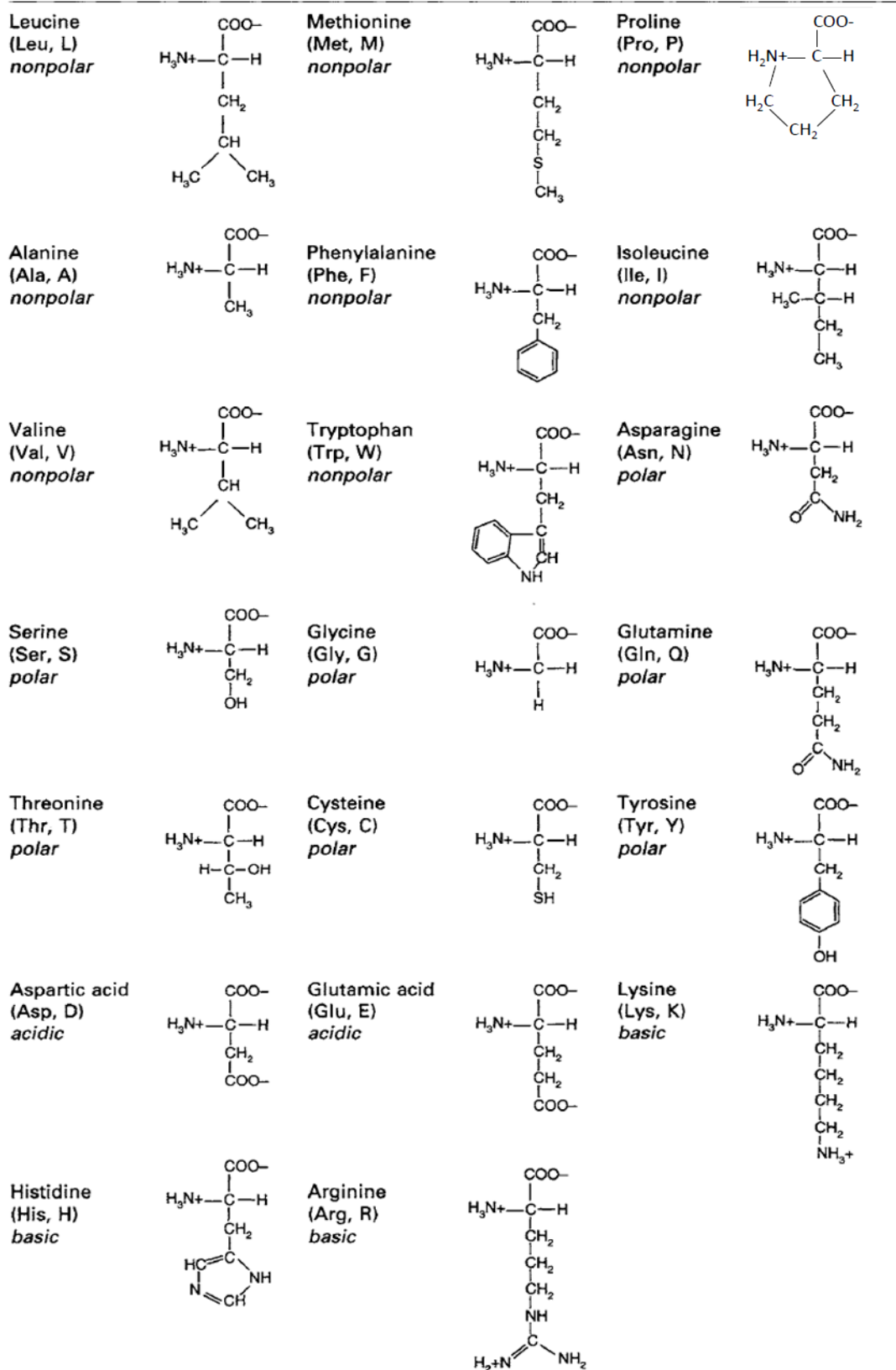
Figure 2.2-2: Backbone structure of the 20 amino acids. Their abbreviations are shown in parentheses. The general chemical character of the side chain is shown in italics [Wie02]
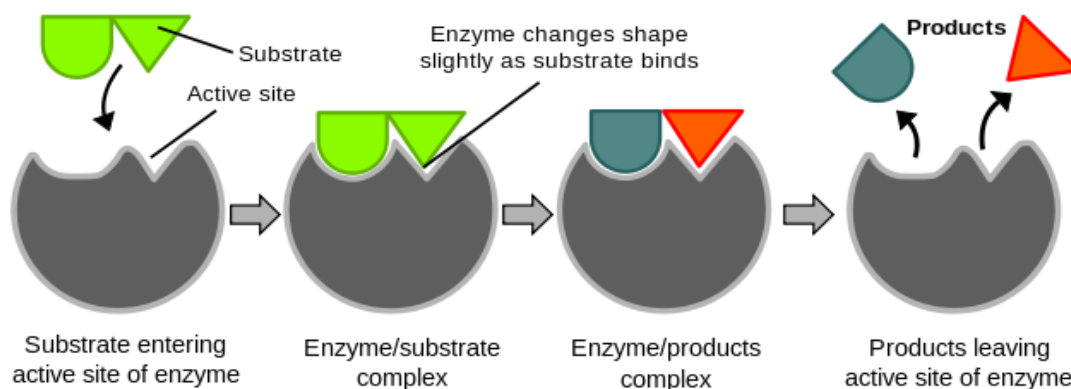
Figure 2.2-3: "The Lock and Key Model" and "Induced Fit Theory" of enzyme action [Enz13]

2.3 Protein Crystallization Techniques and Protein Crystals Structures

As mentioned above, the most important requirement of crystallization in solution is the production of a supersaturation. There is a variety of techniques to bring out a supersaturation in the solution containing a target protein. Table 2.3-1 [Mc99] summaries the common crystallization techniques of attaining supersaturation. Because proteins are the amphoretic molecules, it attempts to crystallize one protein of interest at a pH near its pI to decline the solubility [Wie02]. In addition, precipitant agents, e.g. salts, solvents or polymers, are also effective to alter the protein solubility or the electrolyte properties to let the solution immediately supersaturate with target protein [Mc99].

  For the further industrial scale-up, in the present work, the method of crystallization in solution (batch crystallization) is selected to perform all the crystallization experiments. The method of crystallization in solution requires no complicated procedure more than directly mixing the protein solution with precipitant agents and remaining at a certain temperature to allow crystallization. The method of batch crystallization for protein crystallization has been used for over 150 years [Mc99]. However, this method has not been widely used to screen protein crystallization conditions in the laboratories in recent years because there is a prejudice that batch crystallization is not favorable for small-scale. Additionally, another debate concerning this method is that batch crystallization doesn't provide a slow equilibration to attain high ordered crystals [Mc99]. But there are more than 53 entries

successfully crystallized by batch embodied in NIST/CARB BMC until 1994 [Gil94][Mc99] and this number is increasing annually.

Table 2.3-1: Techniques to attain supersaturation [Mc99]

No.	Crystallization methods
1	Bulk crystallization
2	Batch method in vials
3	Evaporation
4	Bulk dialysis
5	Concentration dialysis
6	Microdialysis
7	Liquid bridge
8	Free interface diffusion
9	Vapor diffusion on plates (sitting drop)
10	Vapor diffusion in hanging drops
11	Sequential extraction
12	pH-induced crystallization
13	Temperature-induced crystallization
14	Crystallization by effector addition
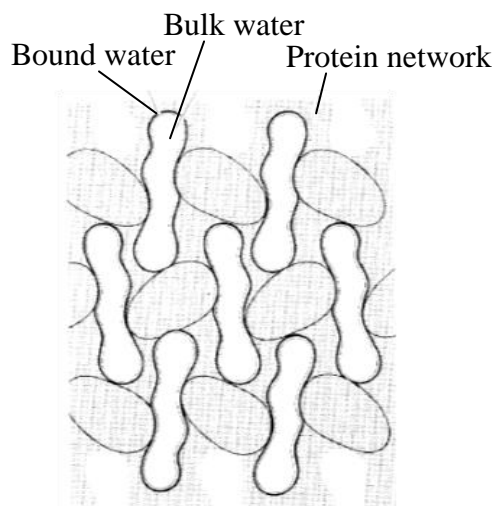
Figure 2.3-1: Structure illustration of protein crystals [Ros86]

It must be taken in account that the structure of protein crystals also differs from the crystals of other common substance. For instance, protein crystals are always composed of 50% or more solvent up to 90% [Mc04]. According to the explanation of Rosenberger [Ros86], as shown in Figure 2.3-1, the formation of protein molecules on the lattice sites is meshwork alike. The bound water in crystal lines the channels and these channels are filled with disordered bulk water which may contain precipitant agents and buffer solution. These specific features of protein crystals result in that protein crystallization will not fit any unmodified inorganic classical growth models.

Jones and Ulrich [Jon10], Müller and Ulrich [Mül11b] had investigated the composition of protein crystals in the case study of lysozyme. It is proven that besides the lysozyme itself the crystals consist of water (in the lattice), salt ions (attaching to the protein molecules) and channels (filling with buffer solution and precipitation agent). This phenomenon shows a fact concerning protein crystals that the crystals of the same protein may possess the same crystal structure, but they should not be called polymorphs due to their different chemical compositions (different buffer and different precipitant agent). Even though a same protein of interest is crystallized with the same initial concentration of buffer solution and the same initial amount of precipitant agent, the content of the buffer and precipitant agent involving in the protein crystals could vary in those crystals forming at a different point of the process. These particular internal compositions of protein crystals result in that the protein crystals could be modified even at the same crystallization conditions. However, in the present work, the distinction of a protein crystal is not that strict and the terminology of the standard industrial crystallization will be used. The modifications by varying crystallization conditions (e.g. different amount of precipitant agent) will only be discussed.

2.4 L-asparaginase II

L-asparaginase II won an attention that benefits from its anti-tumor activity against acute lymphatic leukemia and has been investigated for more than 30 years since in 1976 its positive treatment of remission of acute leukemia in patients was firstly reported [Gru70]. The clinical effect of L-asparaginase II ascribes to its catalyzing function of hydrolyzing L-asparagine, which is a necessary amino acid for the growth of leukemic cell, to aspartic acid. The procedure of the hydrolysis of L-Asparagine is

illustrated in Figure 2.4-1. This hydrolysis function of L-asparaginase II brings the other application of processing aid on food manufacturing, because it is able to reduce formation of acrylamide during heating [Ane11].
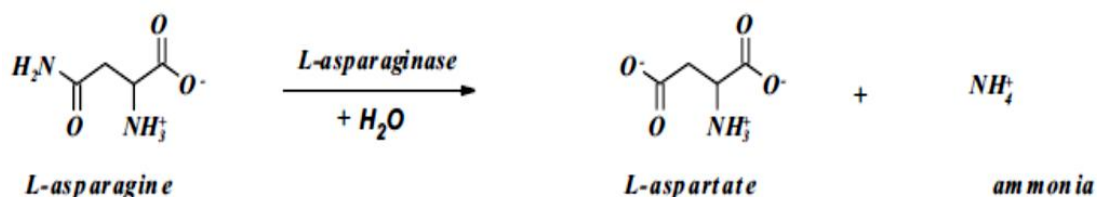
Figure 2.4-1: Schematics of the reaction of L-Asparagine [Bor01]

L-asparaginase II as an enzyme can be obtained from many sources. Available asparaginase can be divided into three families which are a bacterial-type of asparaginase, a plant-type of Asparaginase and the third is an enzyme similar to Rhizobium etli Asparaginase [Bon97]. Bacterial-type L-asparaginase can be further classified into two types: type I and type II. Two types of L-asparaginases, Asn I and Asn II, have been found in *Escherichia coli* K-12. The type II L-asparaginase, which is produced under anaerobic conditions and locats near the cell surface, presents a higher anti-tumor effect than the other [Ced68]. The schematic classification of asparaginase is shown in Figure 2.4-2 [Bor01].
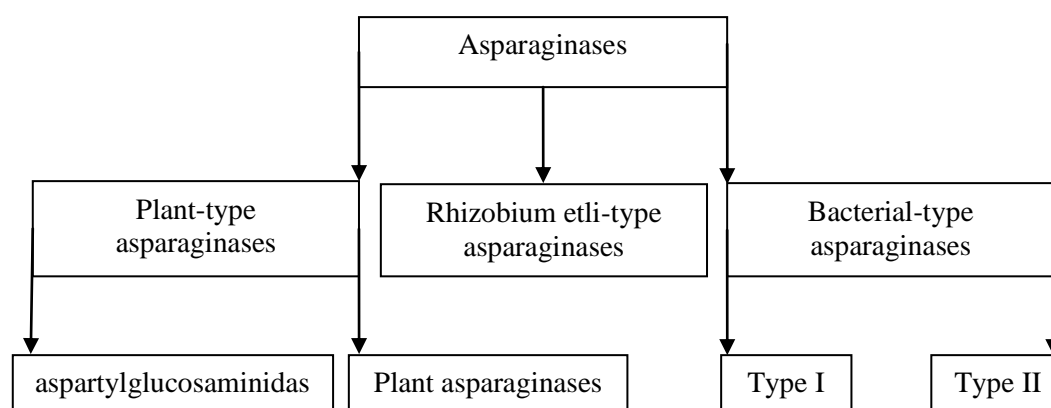
Figure 2.4-2: Classification of Asparaginase [Bor01]

L-asparaginase II is very stable in aqueous solution in the pH range from 5 to 9. At room temperature, the enzyme activity is preserved for weeks under sterile conditions. At higher temperature, for instance, at $60^{\circ}C$, the enzyme loses its activity within 1 h

[Rau70]. But it can be stabilized by addition of glycine and polyethylene glycol (PEG) [Rau70].

The basic properties of L-asparaginase II from *Escherichia coli* are listed in Table 2.4-1.

Table 2.4-1: The basic characters of L-asparaginase II from *Escherichia coli*

Characteristic	Values	Literatures
Molecular weight	142 kDa*	[Pol99]
Iso-electric point	4.9±0.04	[Cam67]
pH optimal	5.0-9.0	[Rau70]
pH range	4.5-11.5	[Ste99]
Special activity	300-625 U/mg	[Coo70]
Temperature of inactivity	60 ^{o}C	[Rau70]
Temperature optimal	0-30 ^{o}C	[Gra72]

*(homotetramer, each monomer is 35 kDa)

Insofar as can be searched from the literatures, the earliest research of L-asparaginase II crystallization was reported in 1969 by Wagner et al. [Wag69], who successfully fractionated and crystallized L-asparaginase II by utilizing PEG. Subsequently, Ho et al. [Ho69] [Ho70] reported a method to purify L-asparaginase II by addition of ethanol. However, this involves multi-processes prior to crystallization, such as, salting out the enzyme and further enriching the enzyme through chromatography. In 1972 Grabner et al. [Gra72] described a simple process to obtain crystalline L-asparaginase II by using ethanol as a precipitant reagent in their patent. However, the detailed information about this process, especially, the process to obtain the crude extract of L-asparaginase II from the harvested cells was not described. Table 2.4-2 catalogues the previous works which are most significant guiding the present work. The raw materials of L-asparaginase II in those works were all obtained from harvested cells of *Escherichia coli*.

Table 2.4-2: Prior arts of L-asparaginase II purification followed by crystallization. (only the arts involving extraction process from *Escherichia coli* and crystallization are denoted)

Material Source	Purification steps prior to crystallization	Crystallization reagents	pH	T/ ℃
Escherichia coli ATCC 9637 [Wag69][Wag71] [Wag73]	Acetone precipitation, urea fractionation	- Add a mixture of PEG_{6000}, water and methanol - Add 2-methylpentane-diol (2,4)	8.5, 5.1	20
Escherichia coli ATCC 13706 [Ho70]	Dialysis, ammonium sulfate fractionation, ethanol fractionation, lyophilize	Add ethanol and magnesium acetate	6.6-6.7	4
Escherichia coli [Gra72]	Salt precipitation	Add cold ethanol (0 ℃)	8.0, 7.4, 5.5, 5.1	5

The trade name of L-asparaginase II as a drug to treat acute lymphocytic leukemia (ALL) is known as Elspar (Merck & Co. Inc., USA).

Figure 2.4-3: Trade name of L-asparaginase II: Elspar [Mem12]

2.5 Aim of This Work

Although the investigations concerning protein crystallization has been done for decades and protein crystals have been successfully obtained at variable conditions,

the knowledge about protein crystallization is still poor. The description offered for the crystallization of conventional molecules is applicable to proteins and enzymes, however, this classical theory does not fulfil all protein systems due to the complexity of protein molecules and the particular composition of protein crystals (see §2.2 and §2.3). The increasing interest of crystallographers in the popular use of protein crystallization serving to produce single crystals (at least 0.5 mm in any dimension) for X-ray crystallography to determine the 3D structure of proteins results in less focus on the fundamentals of nucleation and growth of protein crystals [Wie02]. From the technical level, the bottleneck of determination of protein phase diagrams is that there is large number of parameters, such as pH value, temperature, buffer solution, precipitants, salts supplemented, etc., affecting the phase diagram of each protein [Mc99]. Therefore, the determination of a protein for a phase diagram, taking into account all of the factors as mentioned above, is always time consuming.

Despite various difficulties presented, Miers and Isaac had established a phase diagram for crystallization of a simple chemical system which illustrates the case for concentration as a function of temperature [Mie07]. Lysozyme, the most common object for protein crystallization studies, has possessed a real phase diagram involving multidimensional parameters well established by Cacippo and Pusey [Cac91] [Pus88]. Afterwards, Muschol and Rosenberger [Mus97], Aldabaiben et al. [Ald09], Ryu and Ulrich [Ryu12] completed the phase diagram of lysozyme in details. Lin et al. [Lin08] had also drawn out phase diagrams for the crystallization of some selected proteins, such as lysozyme, catalase (bovine liver), ribonuclease A (type III bovine pancreas), ribonuclease S (bovine pancreas), trypsin (bovine pancreas), concanavalin A (cancanalin ensiformis), Papain (papaya latex), proteinase K (tritirachium album), chymotrypsinogen A (bovine), ELP16 (rattus norvegious). Lin et al. [Lin08] performed the crystallization by a vapour diffusion method in a hanging drop at different temperatures. The nucleation and precipitation curves were determined by microscope at 50-fold magnification. The solubility curves were determined by titration of the residue protein concentration in equilibrium with crystals after 50 days. The disadvantage of this method is that the measurements are offline and it mostly depends on the observation by naked eyes.

Based on the reasons described above, the present work emphasizes to produce L-asparaginase II crystals by the simple crystallization method in solution and then to produce a phase diagram which can serve for crystallization of L-asparaginase II. The

metastable zone width (MZW) in the presence of a given precipitant agent will be measured, too. Here an online turbidity technique was applied to determine the nucleation temperature and solubility temperature simultaneously through variation of the temperature. Thirdly, the X-ray diffraction technique was utilized to identify the internal structure of crystalline L-asparaginase II formed with different precipitant agents, respectively. More important, the raw materials of L-asparaginase II were fresh extracted from a recombinant *Escherichia coli* cells rather than purchase from a company, which allows a better understanding of the crystallization behavior from the source.

3. MATERIALS AND EXPERIMENTAL METHODS

3.1 Materials

3.1.1 L-asparaginase II

L-asparaginase II was extracted from frozen recombinant *Escherichia coli* cells which were kindly provided by the group of Prof. Dr. Markus Pietzsch (Institute of pharmacy, Department of downstream processing). The cells were cultivated according to the description of Müller et al. [Mül11a] with the following modifications: the cells were grown in a fed-batch with an initial culture volume of 11.5 L medium and with a start concentration of 20 g/L glucose at 37 °C. After 8.5 h the enzyme production was induced by addition of 1 mM IPTG. The cultivation was continued for 3 h. The medium was prepared following Wilms et al. [Wil01]. The biomass was harvested by a centrifuge Z41 (Carl Padberg, Germany), washed with 0.9% NaCl solution and finally stored at -80 °C before using.

3.1.2 Chemical materials and apparatus

The information of chemical materials, solutions and equipments that used in this work is summarized as follows (Table 3.1-1, Table 3.1-2 and Table 3.1-3).

Table 3.1-1: Chemical Materials used in Experiments

Name	Producer	Art.-No.	Lot.-No.	Purity
Tris Ultra Qualität	Carl Roth GmbH & Co. KG, Karlsruhe	5429.3	49574655	≥99.9%
Acetic acid	Carl Roth GmbH & Co. KG, Karlsruhe	3738.4	12677596	100%
Acetone	Carl Roth GmbH & Co. KG, Karlsruhe	9372.6	069103058	≥99.8%
L-asparagine Monohydrate	Sigma-Aldrich Chemie GmbH & Co KG, Steinheim		90811015	99%
Ethanol	Carl Roth GmbH & Co. KG, Karlsruhe	P076.1	589941	≥99.9%

2-methyl-2,4-pentandiol (MPD)	Carl Roth GmbH & Co. KG, Karlsruh	CN17.2		≥99%
PEG$_{6000}$	Carl Roth GmbH & Co. KG, Karlsruhe	0158.4	40894408	
TCA (Trichloroacetic acid)	Sigma-Aldrich Chemie GmbH & Co KG, Steinheim	T9159-100G	039K1648	≥99%
Nessler's Reagent	Sigma-Aldrich Chemie GmbH & Co KG, Steinheim	72190	SZE92790	
BSA (Albumin from Bovine Serum)	Fluka Chemie GmbH CH-9431 Buchs	05488	S27641116	≥ 96%
Protein molecular weight marker	Fermentas GmbH (St. Leon-Rot)	#SM0431 #SM0661		
Brilliant Blau G-250	Carl Roth GmbH & Co. KG, Karlsruhe	9598.2		
N,N'-methylbis-acrylamide	Carl Roth GmbH & Co. KG, Karlsruhe	7867.1	48575599	2×crys.
Sodium azide	Carl Roth GmbH & Co. KG, Karlsruhe	K305.1	05676218	≥99%
Acrylamide	Carl Roth GmbH & Co. KG, Karlsruhe	7871.2	05676126	≥98%
SDS	Carl Roth GmbH & Co. KG, Karlsruhe	2326.1	14678255	≥99%
Bromphenol blue	Fluka Chemie GmbH CH-9431 Buchs	18030	417639/1 41006121	
Glycerol	Carl Roth GmbH & Co. KG, Karlsruhe	3783.1	17896047	≥99.5%
Glycine	Merk Schuchardt OHG, Hohenbrunn	8.16013.-100	S3930513337	≥99%
2-Propanol	Carl Roth GmbH & Co. KG, Karlsruhe	7343.2	908891	≥99.9%
Ammonium peroxodisulphate (APS)	Carl Roth GmbH & Co. KG, Karlsruhe	9592.2	48575673	≥98%

TEMED	Alfa Aesar Gmbh & Co.KG, Karlsruhe	A12536/ L00847	FA013272	≥99%
2-mercaptoethanol	Carl Roth GmbH & Co. KG, Karlsruhe	4227.1	03782687	≥99%

Table 3.1-2: Recipe of Solutions used in Experiments

Name	Concentration	pH	Weight in a final vol. of 1 L
Tris-HCl buffer	0.05 M	8.6	6.057 g (Tris)
Tris-acetate buffer	0.05 M	5.1	2.86 mL (acetic acid)
L-asparagine Monohydrate	1.5 mg/mL		1.5 g
TCA	1.5 M		245.1 g
$^{50\%}PEG_{6000}$	50% (w/v)		500 g

Table 3.1-3: Equipments

Name	Type	Producer
High Pressure Homogenizer	APV-2000	Invesys APV Products, Arbertslund, Dänemark
Digital Microscope	VHX-500F Zoom ×100~×1000	KEYENCE, Osaka, Japan
UV VIS Spectrophotometer	SPECORD® 40	Analytik Jena AG
Spectroanalyse-software	WinASPECT®	Analytik Jena AG
Centrifuge	SIGMA 2-16 K Avanti™, J30l	Sigma, D-37520 Osterode am Harz, Germany Beckmann Coulter GmbH, Krefeld, Germany
Pipette	2-20 μL 20-200 μL 100-1000 μL 500-5000 μL	Eppendorf AG, Hamburg, Germany

pH-meter	inoLab pH level 2, pH 523	Wissenschaftlich-Technische Werkstätten, Weilheim, Germany
UV Cuvette	70 μL micro, 12.5×12.5×45 mm	BRAND GmbH & Co. KG
PMMA Cuvette	2.5 mL	Carl Roth GmbH & Co. KG, Karlsruhe, Germany
Microplate	96-well, PS	Carl Roth GmbH & Co. KG, Karlsruhe, Germany
Ultrafree-CL centrifugal filter unit	PVDF microporous membrane, 0.45 μm	Millipore, Billerica, MA, USA
SDS-PAGE mighty small apparatus		Hoefer, Amersham Biosciences, Freiburg, Germany
X-ray Powder Diffraction (XRPD)	Bruker D4 Endeavor diffractometer Bruker D8 ADVANCE	Bruker, Karlsruhe, Germany Bruker, Karlsruhe, Germany
Single Crystal X-ray diffraction	AFC-11, CCD Saturn 944+	Rigaku/MSC, Tokyo, Japan
Cryoloop		Hampton Research, USA
Turbidity system	RS-10 Reaction Station	ThermoAnalytic Instrument, Berlin, Germany
IR-probe	DipTip^{TM}	World Precision Instruments, Inc.

3.2 Experimental Methods and Procedures

3.2.1 L-asparaginase II extract from *Escherichia coli* biomass

The developed process of enzyme extraction from *Escherichia coli* was based on the patent of Wagner et al. [Wag73]. 51.2 g frozen cell cakes of *Escherichia coli* BL21Gold pET11a-ansB (kept at -80°C, shown in Figure 3.2-1) were suspended in 256 mL distilled water. Such suspension was treated by ultrasonic for ~ 30 s and the cells in the suspension were disintegrated by a high pressure homogenizer at 1000 bar,

in 4 cycles (the collection beaker for each cycle must be kept in ice). The high pressure homogenizer creates conditions of high turbulence and shear, combined with compression, acceleration, pressure drop, and impact causing the disintegration of particles and dispersion throughout the product [Nir09]. Then 1232 mL cold acetone (at 4°C) was added. After the centrifugation (10000g, 30 min, 4°C), the precipitate was collected and resuspended again in 256 mL distilled water. During the stirring the suspension was adjusted to pH 7.5-7.8 with a base. A precipitate was formed and was centrifuged away (14000g, 30 min, 4°C). Another cold acetone (at 4°C) which was four times volume of the supernatant was added to the remaining supernatant to form a precipitate which was centrifuged again. The resulting precipitate was suspended in Tris-acetate buffer of initial concentration of 50 mM pH 5.1 to a final suspension of 5% (or 10%, w/v), and the insoluble stuff was removed by centrifugation. The collected supernatant was the protein solution of L-asparaginase II for the utilization in further crystallization experiment.

Figure 3.2-1: Frozen biomass of *Escherichia coli* containing L-asparaginase II

3.2.2 Protein Assay by Spectrophotometer measurement

In this work, the enzymatic activity and protein concentration were calculated from the absorbance value of protein solution measured by spectrophotometer. Spectrophotometer is a technique to measure the light intensity. The most common application of spectrophotometer is the measurement of light absorbance at a given wavelength. Normally, a spectrophotometer consists two parts, that is, a spectrometer for producing a beam of light and a photometer for measuring the intensity of light.

Usually, a cuvette containing the liquid of sample is placed between the spectrometer and photometer. The amount of light passing through the cuvette is measured by the photometer. The light absorbance can be read in a display device. The drawing of mechanism of the spectrophotometer is shown in Figure 3.2-2 [Spe10].
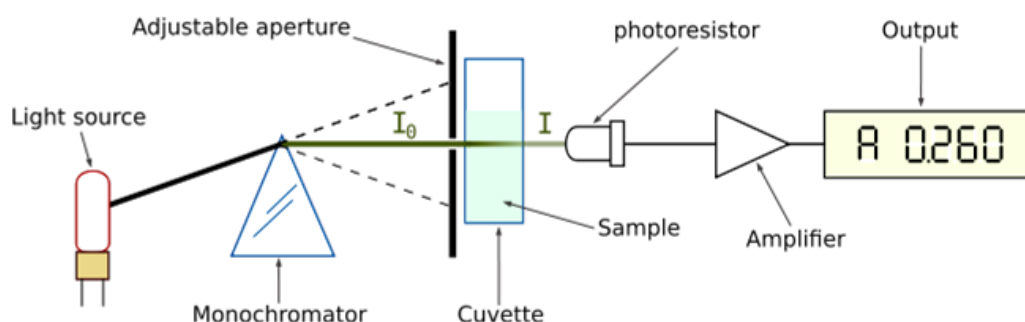
Figure 3.2-2: Drawing of the mechanism of single beam spectrophotometer [Spe10]

The measurement of light absorbance is based on the Beer-Lambert Law. The absorbance (also can be replaced by extinction) of liquid sample can be written in Equation 3.2-1 [Bee14]:

$$A = -log_{10}\left(\frac{I}{I_o}\right) = \varepsilon cd \tag{3.2-1}$$

I_o and I indicate the intensities of light before and after passing through the cuvette, respectively. ε is the molar extinction coefficient; c is the concentration of sample solution [mol/L]; d is the thickness of the cuvette which the light beams passing through [cm]. That means the absorbance becomes linear with the concentration during this way.

➤ *Activity test*

The absorbance maximum under UV light only can indicate the roughly purity of protein, whereas the activity of protein evaluates the protein properties by exact values, not to mention the specific activity. Generally, a specific activity, a characteristic property of a pure enzyme, typifies the catalysis capacity of protein. Specific activity is expressed as units per mg of protein or solids as indicated [Ho70] (see Equation 3.2-2).

$$\textbf{\textit{Specific activity}}\left(\frac{U}{mg}\right) = \frac{Activity\ [\frac{U}{mL}]}{Protein\ concentration\ [\frac{mg}{mL}]} \tag{3.2-2}$$

According to Equation 3.2-2 of calculating specific activity, the measurements of both of enzyme activity and protein concentration are required.

As mentioned before, L-asparaginase II can catalyze the hydrolysis reaction of L-asparagine monohydrate to produce L-aspartic acid and ammonia. Here the activity capacity of L-asparaginase II as an enzyme was determined by Nesslerization (color developer) of the ammonia liberated from the hydrolysis, as the ammonia concentration increases the color of reaction solution darkens [Mas63].

Before the enzyme assay, a calibration curve of ammonia must be plotted. A dilution series of ammonium sulfate solution were prepared in the range of 0-0.9 μmol/mL in steps of 0.1 μmol/mL with distilled water. 100 μL each sample solution were mixed with 1400 μL distilled water and 200 μL Nessler's reagent in a UV cuvette. After standing for 10 min, absorbance measurement was performed at 436 nm by a UV-spectrophotometer. The calibration curve was obtained by plotting the amount of ammonia in μmol against the absorbance values.

The reaction for activity assay with Nessler's reagent was carried out by a modified method based on the description of Mashburn and Wriston [Mas63]. 100 μL of 50 mM Tris-HCl buffer pH 8.6 mixed with 850 μL 1.5 mg/mL L-Asparagine monohydrate (must be fresh prepared each time with the same buffer) in a Eppendorf Eppi, keeping in thermo block at 37°C prior to react. For each sample, a blank reference without librated ammonia should be prepared by adding 50 μL TCA solution before adding diluted L-asparaginase II solution. The reaction started by adding 50 μL diluted L-asparaginase II solution in both blank and sample, respectively. After 10 min, the reaction was stopped by adding 50 μL of TCA (no TCA was added to the blanks after reaction). All operations were conducted in the thermo block in order to maintain a constant temperature at 37°C. After the reaction stopped, centrifugation was carried out for short time to remove the insoluble particles and then 100 μL of clear supernatant of this reaction solution was taken out and added to 1400 μL distilled water in a UV cuvette as well as with 200 μL Nessler's reagent. The absorbance of such mixture was read by spectrophotometer at 436 nm. At this time the activity of L-asparaginase II could be finally calculated by Equation 3.2-3:

$$\boldsymbol{Activity\ \left(\frac{U}{mL}\right)} = \frac{\frac{E_{436}}{F} \times V_{test}[\mu L] \times dilution}{reaction\ time\ [min] \times V_{reaction}[\mu L] \times V_{enzyme}\ [mL]} \qquad \textbf{(3.2-3)}$$

F: slope of ammonium sulfate calibration curve

V_{test} = 1050 μL

$V_{reaction}$= 100 μL

V_{enzyme}= 0.05 mL

Here, the activity value is expressed in the unit U. 1U represents the amount of L-asparaginase II which catalyses the formation of 1 μmol ammonia per minute at 37 ^{o}C [Ho70].

➢ ***Bradford test for protein determination***

Bradford test [Bra76] possessing the high-sensitivity of ~1 μg is in favor to estimate the protein concentration in the present work. This method relies on monitoring the increase in the absorbance at 595 nm because of the binding of the dye Commassie Brilliant Blue G-250 to proteins [Bra76]. In order to prepare the dyeing reagent, 100 mg Coommassie-brilliant blue G-250 are dissolved in 50 mL 95% ethanol (w/v). Then 100 mL 85% phosphoric acid (w/v) was added. The total volume was filled up with distilled water until 600 mL. The solution is filtrated afterwards. After addition of 100 mL glycerol fill it up to 1 L with distilled water. The reagent can be used after storing for 24 hours. 50 μL diluted sample solution was added into 2 mL such dyeing reagent in. The absorbance at 595 nm of the mixture is read by a spectrophotometer after 5 min but not longer than 10 min. A calibration curve of a standard protein of bovine Serum Albumin (BSA), ranging from 0 to 1 mg/mL in steps of 0.1 mg/mL, must be fresh obtained in every cycle of measurement. Weber [Web08] has declared that there are no measurable differences in the values whether the standard protein of BSA dissolved in water or in a phosphate buffer (pH 6.5). Here, the BSA powder was dissolved in the same buffer solution as the protein sample solution. BSA standard solution as well as the protein sample solution was diluted with distilled water. The protein concentration of each sample can be calculated by Equation 3.2-4. Factor is the slope of the calibration curve of BSA.

$$\boldsymbol{Protein\ concentration}\ \left[\frac{\boldsymbol{mg}}{\boldsymbol{mL}}\right] = \frac{\boldsymbol{E_{595}}}{\boldsymbol{Factor}} \times \boldsymbol{dilution} \qquad \textbf{(3.2-4)}$$

3.2.3 Sodium dodecyl sulfate polyacrylamide gel electrophoresis (SDS-PAGE)

SDS-PAGE method is a visual analytical technique to evaluate the impurities or foreign proteins in the samples. The solutions required for the SDS-PAGE were prepared as follows [Web08]:

Separating Gel buffer:

- 18.18 g Tris

- 0.4 g SDS

- 100 μL 10% NaN_3

- fill up to 80 mL with distilled water

- adjust pH value to 8.8 with 4 M HCl

- fill up to 100 mL with distilled water

Stacking Gel buffer:

- 6.06 g Tris

- 0.4 g SDS

- 100 μL 10% NaN_3

- fill up to 70 mL with distilled water

- adjust pH value to 6.8 with 4 M HCl

- fill up to 100 mL with distilled water

30% acryl-/bisacrylamide solution:

- 29.1 g acrylamide

- 0.9 g N, N'-methylbisacrylamide

- fill up to 100 mL with distilled water

Sample buffer:

-2.72g Tris, 5 g SDS, 50 mg Bromphenol blue and 50 g Glycerol in 95 mL distilled water

- adjust pH to 6.8 with HCl

- fill up to 100 mL with distilled water

Cathode buffer:

- 30.28 g Tris

- 144 g Glycin

- 10 g SDS

- 1 mL 10% NaN$_3$

- fill up to 1 L with distilled water

Dyeing reagent:

- 1 g Coomassie Brilliant Blue G-250 dissolved in 700 mL distilled water and stirred until dissolve

- 200 mL 2-propanel

- 100 mL acetic acid

- filter with a filter paper

Discoloring solution:

- 200 mL 2-propanol

- 100 mL acetic acid

- fill up to 1 L with distilled water

Table 3.2-1: Preparation of mixing separating gel with stacking gel [Lae70]

	2 separating gels (12.5%)	2 stacking gels (4.5%)
Gel buffer	2.5 mL	1.25 mL
Acry-/ bisacrylamide	4.2 mL	0.75 mL
Distilled water	3.3 mL	3 mL
TEMED	10 μL	10 μL
Saturated APS (ammonium peroxodisulphate)	20 μL	20 μL

The electrophoresis experiments (including casting the gels and running the electrophoresis) were operated according to the description of Laemmli [Lae70] by using a Mighty Small apparatus from Höfer (Amersham Biosciences). The gels consisted of a resolving (12.5% acrylamide) covered by a stacking (4.5% acrylamide)

gel, see Table 3.2-1. The procedure including producing the SDS-PAGE gel and performing the electrophoresis is illustrated in Figure 3.2-3. The samples need to be evaluated were diluted with distilled water and were added to SDS-sample buffer (normally at 1:1), then were preheated at 99 ^{o}C in a thermo block for 5 min. It must keep in mind that 1 mL SDS-sample buffer needs to be added into 10 μL 2-mercaptoethanol just before use. The standard molecular weight maker (5 μL) and each sample (10 μL) were loaded onto the gels, respectively. After finishing the electrophoresis, the gels were removed from the apparatus and were stained with the prepared dyeing reagent. After destaining, the gels were dried between two cellophane foils fixed in a frame at room temperature for 3 days.

Electrophoresis means the migration of charged particles in an electrical field according to their net electrical charge, shape and molecular weight. During SDS-PAGE (an anionic detergent) the secondary and non-disulfide-linked tertiary structures were denatured, and a negative charge was loaded to each protein chain. In this way, SDS gives a uniform surface charge ratio to the protein along the length of the polypeptide. Thus proteins migrate in electrical field only according their molecular weight [Ele10]. As a result, proteins can be separated in gels depending to their molecular weight.
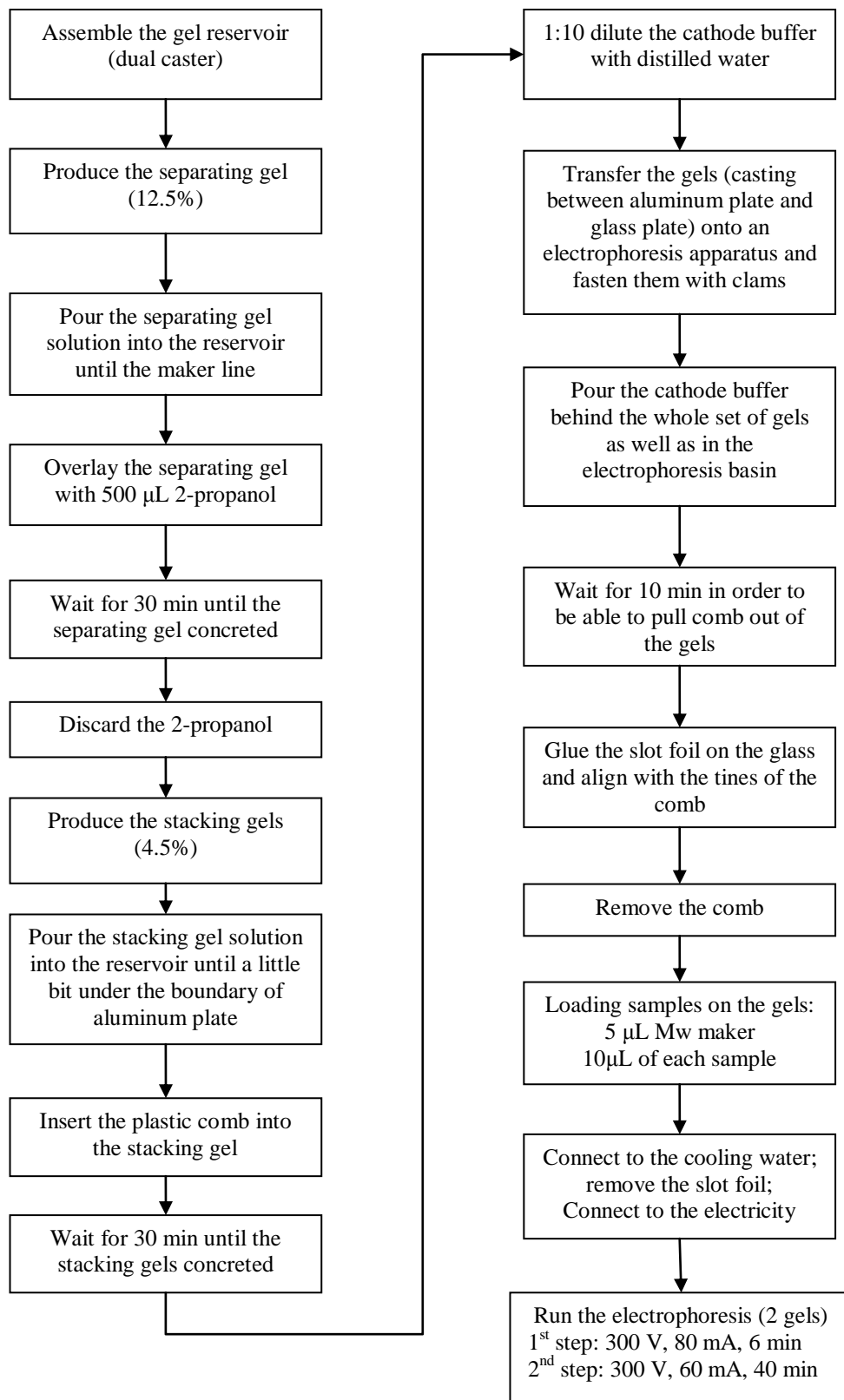
Figure 3.2-3: Illustration of the procedure of producing SDS-PAGE gels and running the electrophoresis

3.2.4 Crystallization in solution

In most literatures, the vapor-diffusion method is, such as hanging-drop and sitting-drop, frequently used to produce a single crystalline L-asparaginase II for further single crystal X-ray diffraction [Swa93][Pol99][Koz02]. But in this case, the amount of crystals is pursued for the following analysis. Thus, in the present work, the method of crystallization in solution, which was developed from the works of Grabner et al. [Gra70], Ho et al. [Ho70] and Rauenbusch et al. [Rau70], was favored to produce larger amount of crystals and to serve as the materials for the further investigation on crystallization behavior. Consequently, the small scale crystallization methods such as evaporating methods were not considering.

It is known that PEG belongs to the long chain polymers, while ethanol belongs to the category of volatile organic solvents [Mc04]. Another typical precipitant agent widely used in the protein crystallization is 2-methyl-2, 4-pentandiol (MPD), which is classed as the low molecular weight polymers and non-volatile organic compounds [Mc04]. Theoretically, PEG with molecular weight 4000 or 6000 is more effective for most protein systems [Wie02]. In present work, PEG_{6000} was favored. Therefore, PEG_{6000}, ethanol and MPD were chosen as the precipitant agents to induce the crystallization in the current work. PEG_{6000} was added to the protein solution in the form of 50% (w/v) solution in distilled water in order to reduce its viscosity. The details of experimental process was summarizing in Table 3.2-2.

Table 3.2-2: Crystallization in solution supplemented with PEG_{6000}, ethanol and MPD

	PEG₆₀₀₀	Ethanol	MPD
Protein solution	L-asparaginase II solution in an initial 50 mM Tris-acetate buffer pH 5.1	L-asparaginase II solution in an initial 50 mM Tris-acetate buffer pH 5.1	L-asparaginase II solution in an initial 50 mM Tris-acetate buffer pH 5.1
Precipitant agent	PEG_{6000}	ethanol (6-8 ^{o}C)	MPD (6-8 ^{o}C)
Centrifuge	remove insoluble particles by centrifuging	remove insoluble particles by centrifuging	remove insoluble particles by centrifuging
Crystallzation Temperature	Room temperature or 8 ^{o}C	8 ^{o}C	8 ^{o}C

In order to detect the crystallization situation conveniently, after insoluble particles removing, the mixture was loaded in a 96-well microplate (200 μL in each well) and such microplate was kept at designed temperature with a film and the plastic cover to prevent from solvent evaporation.

Figure 3.2-4: 96-well microplate from Carl Roth (Article 9291.1) [Car11]

3.2.5 Determination of phase diagram including metastable zone width by a turbidity technique

> *Apparatus and principle of online turbidity measurement*

The working principle of this online turbidity technique is based on detecting the turbidity changes of the sample solution with knowing concentration through

temperature variation. The biggest advantage of this technique is that, comparing with the conventional method, it is possible to determine both nucleation and solubility points expressed in temperature simultaneously in one online measurement through cooling / heating the sample solution.

The online measurement was performed in a RS-10 System (as shown in Figure 3.2-5) from Thermoanalytic Instruments (Berlin, Germany). This system involves three main parts, that is, a reaction station with 10 cells, a multi-temperature unit and a multi-IR box. The reaction station allows performing 10 measurements at the same time. Each cell can be heated / cooled and stirred independently of the cell next to it. The operation temperature is allowed setting from -30 to 150 ℃. The cooling / heating rate is up to 5 K/min. The range of stirring speed is from 250 rpm to 1200 rpm. The multi-temperature unit also involves 10 sockets and each is directly connecting to a temperature sensor dipping into the test solution to monitor the real temperature of the solution. The multi-IR box plays a role as an emitter as well as a receiver to detect the turbidity changes of the sample solution when an IR probe (World Precision Instruments, USA) is immersed into the solution. The IR probe is designed as a miniature transmission probe and the operation wavelength range of the emitted light through the probe is 920-960 nm. The structure as well as the work principle of the IR probe is illustrated in Figure 3.2-6.

In order to identify the nucleation temperature and solubility temperature of a given sample solution, the solution is cooled down firstly and then is heated up again. The IR signal (transmission) of the sample solution at each temperature is online read by RSPC control software in a double Y-axis interface plotting IR-reading (transmission) and temperature versus the elapsed time. The value of IR reading with respect to the transmission of the sample solution is the highest at the beginning of one measurement when the sample solution is clear. As the solution is cooled down and reaches the temperature of spontaneous nucleation, the IR reading decreases resulting from light scattering by crystals. During the heating process, the transmission in the sample solution increases again due to dissolution of the crystals and the solubility temperature at which the transmission comes back the highest plateau can be determined.

> *Online turbidity measurement*

A glass test tube containing 7-15 mL sample solution, mixing of initial L-asparaginase II solution and one precipitant agent, was placed in a cell of the RS-10 reaction station. A magnetic stirrer was added to agitate the solution during measurement with a speed of 500-800 rpm applied on the solution mixed with ethanol, 500-1000 rpm applied on that mixed with PEG_{6000} and 600-700 rpm applied on the sample solution supplemented with MPD. The measurement was carrying out when the IR probe and the temperature sensor were immersed into the solution. The operation temperature was set, for instance, in Figure 3.2-7, at 30 ℃ firstly and kept for 30 min, in order to let the solution reach the set temperature. Then the temperature decreased to 1 ℃ at a cooling rate of 0.1 K/min. The nucleation point could be defined when the IR-reading signal started to decline in cooling process (as shown in Figure 3.2-7, nucleation). After maintaining at 1 ℃ for ~150 min that allowed nuclei formation and growth, the temperature increased by the same speed up to 35 ℃. The crystals in the solution dissolved during heating and the solubility point could be clarified when the curve of IR-reading (transmission) came back the highest value to a plateau (as shown in Figure 3.2-7, solubility). One cycle measurement going through nuclei nucleation and crystals dissolution takes up 13-14 hours and this period could be shorten by writing the temperature program.
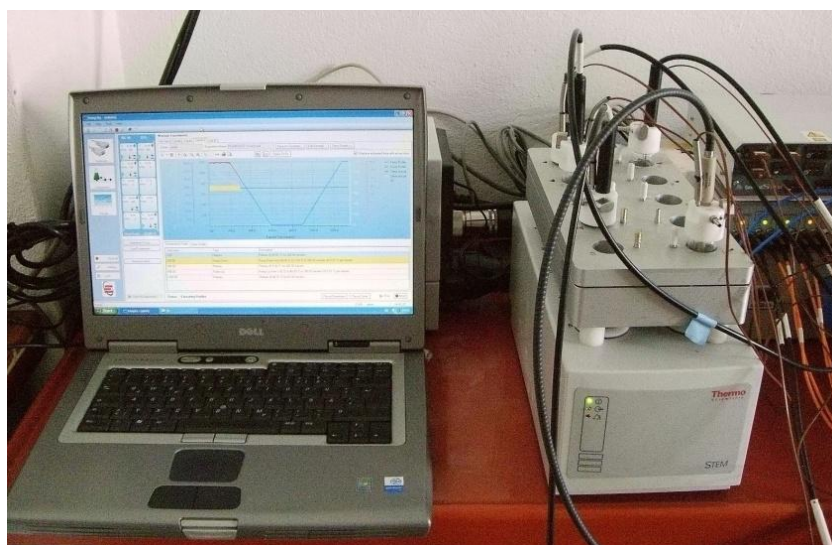

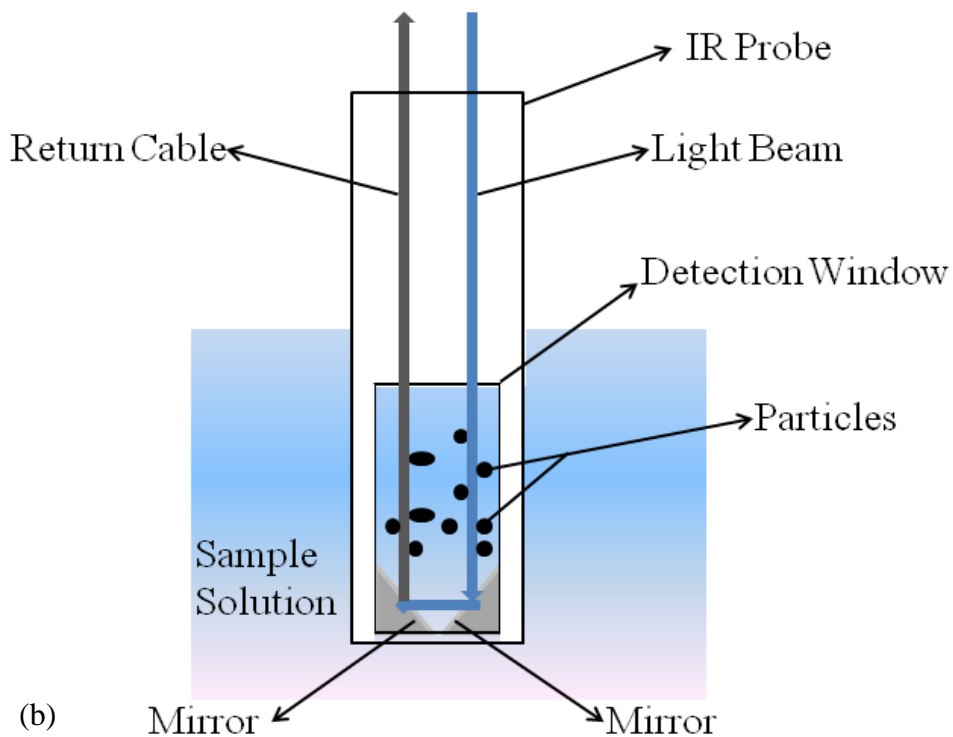**Figure 3.2-5:** RS-10 System from ThermoAnalytic Instruments
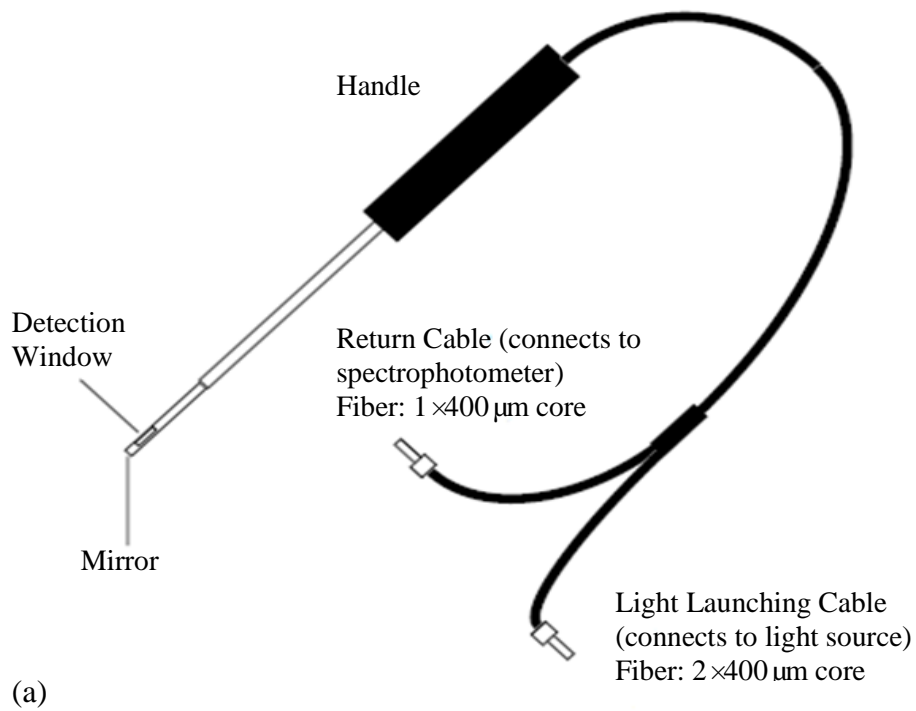
Figure 3.2-6: The illustration of IR probe (World Precision Instruments, Inc., USA). (a): the outline of an IR probe; (b): internal structure of IR probe and its work principle
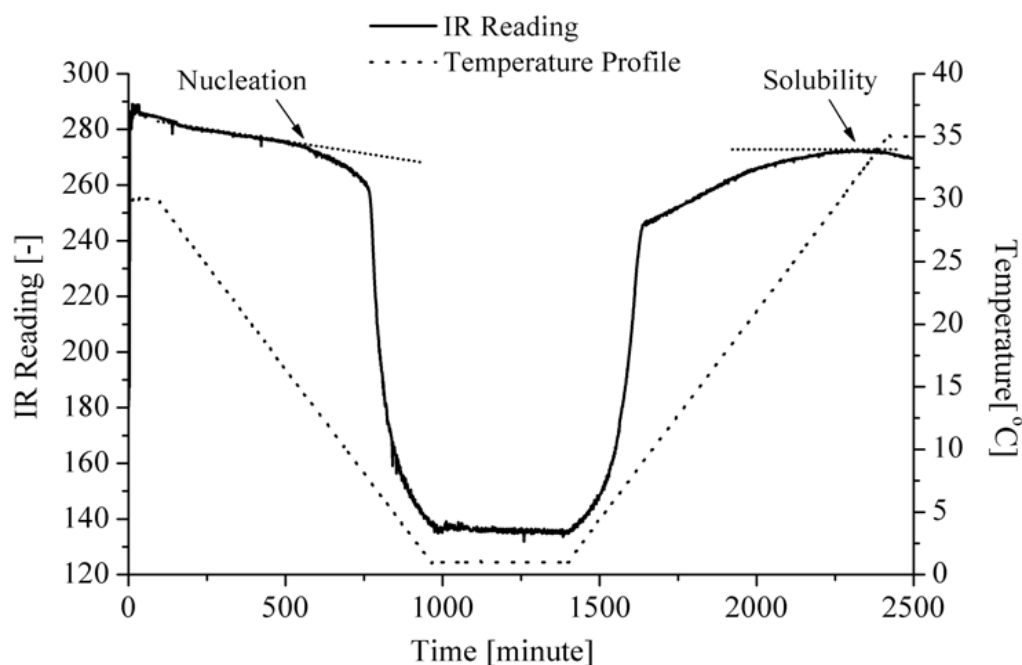
Figure 3.2-7: Illustration of the interface of the turbidity measurement on the PC. Temperature profile: 30 ℃ - 1 ℃ - 35 ℃, cooling rate / heating rate: 0.1 K/min, stirring speed: 600 rpm. Protein concentration: 0.65 mg/mL, in 50 mM (initial concentration) Tris-acetate buffer solution at pH 5.1, MPD concentration of 28.6% (v/v)

The protein concentration, regarding the sample solution supplemented with PEG$_{6000}$ or ethanol, was determined by a Bradford assay after adding PEG$_{6000}$ or ethanol, because there were insoluble particles forming after adding PEG$_{6000}$ or ethanol in the L-asparaginase II solution. Those insoluble particles were removed by centrifugation immediately. Therefore, the protein concentration of each sample solution cannot be calculated on the basis of the original protein concentration of L-asparaginase II solution. It has been verified that the presence of 95% ethanol (initial concentration) has no interference of the Bradford assay [Bra76]. On the other hand, according to the description of González et al. [Gon11], the Bradford assay can be applied in principle when the content of PEG (Mw 400-20000) is diluted less than 1% prior to mixing with dyeing solution. In the present work, the sample solution for Bradford assay was diluted to attain ethanol concentration of 0.52-1.14% (v/v) and PEG$_{6000}$ concentration of 0.16-0.33% (w/v). Thus, the minor presence of ethanol or PEG$_{6000}$ has no influences on the protein assay. As to the sample solution supplemented with MPD, the protein concentration was calculated based on the original protein concentration of L-asparaginase II solution which was determined

37

prior to mixing of MPD. Because there were no evident insoluble particles forming after adding MPD in the L-asparaginase II solution, the centrifugation was not carried out on this sample.

In the activity test performed by Nesslerization [Mas63], each sample was measured against one own blank which contained same concentration of additives as its corresponding sample, respectively.

3.2.5 X-ray diffraction Analysis

X-ray diffraction is an effective technique for crystallography analysis. Since the successfully experiment of X-rays by W. L. Braggs in 1912 [Bra12], who described that the X-ray diffraction was able to utilized to determine the atomic structure of matters and deduced the famous Bragg Equation (as shown in Equation 3.2-5), X-ray diffraction has been carried out to determine the atomic structure of conventional substances. The first protein structure of myoglobin determined by X-ray crystallography was obtained in 1958 by M. Perutz and J. Kendrew, who won the Chemistry Nobel Prize in 1962 [Ken58]. X-rays are electromagnetic waves with shorter wavelength of ~ 1 Å than the visible light with wavelength of 4000-7000 Å [Din08]. Because the wavelength of X-rays is typically the same order of magnitude as the spacing of parallel lattice planes of crystals, diffraction pattern could be produced when the X-rays impinge on the regular array of atoms.
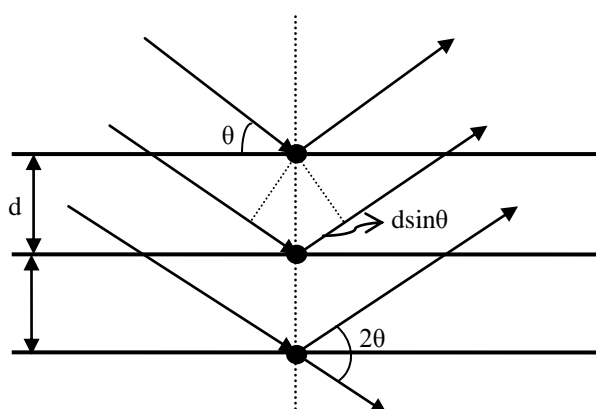

Figure 3.2-8: The illustration of Bragg's low. d: the spacing between the planes in the atomic lattice; 2θ: the diffraction angle

As shown in Figure 3.2-8, the planes in a crystal can be considered the semi-transparent mirrors. When the X-rays beam with a wavelength similar to the distance

between the planes in a crystal hits the crystal, the X-rays are scattered by electrons bound to the atoms. The atoms in a regular array will produce spherical waves. Some waves are in sync in a few specific directions satisfying the Bragg Equation (as shown in Equation 3.2-5). These reflection waves in such specific directions could be collected by a detector and appear as spots on the diffraction pattern [Din08]. From the positions of reflection spots on the pattern, the spacing of atoms in the crystal structure could be learned. The location of each atom in the crystal structure could be calculated by the electron density resulting from the intensities of the spots and then the model of a inter structure of a crystal is able to be built [Kar14].

$$n\lambda = 2d\sin\theta \qquad\qquad (3.2\text{-}5)$$

A single crystal with enough size (at least 0.01mm in all dimensions) and good symmetry (no twinning and no polycrystalline) provides full information of the internal structure and internal compositions determined by X-ray diffraction. However, such perfect single crystal is not always obtained. In this case, the technique of X-ray Powder Diffraction (XRPD) is a good substitute. The sample for XRPD measurement is the powder in milligrams consisting of many grinded crystals with a size of 0.005mm in all dimensions [Dep06]. But the big limit of XRPD compared with X-ray diffraction on single crystal is crystal structure determination. On the other hand, XRPD offers the advantage to identify each phase from a multi-phase powder sample in its X-ray pattern.

In the present work, X-ray diffraction on a single crystal was preferred to determine the internal structure of the protein crystals obtained from the crystallization in solution involving a given precipitant agent. Nevertheless, XRPD was also chosen as an alternative technique if single crystals are not available.

> ➤ *Single Crystal X-ray Diffraction*

In the present work, the crystals obtaining from solution crystallization experiments supplemented with different precipitant agents were detected by single crystal X-ray diffraction, respectively. The crystals for the measurement of single X-ray diffraction were mounted from mother liquor by a cryoloop (Hampton Research, USA). The diffraction data were collected at 100K by using a Satum 944+ detector (CCD++, Rigaku/MSC, Japan) and a CuKα rotating anode with wavelength of λ=1.5418Å

generated by a MicroMax007 generator (Rigaku/MSC, Japan) operated at 40 kV and 20 mA (max. power 0.8 kW) with 0.5 ° oscillation.

> ### *X-ray Powder Diffraction (XRPD)*

The sample for the X-ray Powder Diffraction was collected from mother liquor by centrifuging in an Ultrafree-CL centrifugal filter unit with PVDF microporous membrane, pore size of 0.45 μm (Millipore, USA). The crystals were collected and were kept at 8 ℃ overnight until they were dry. After that, the dry crystals were grinded to fine powder with an agate mortar and pestle. The fine powder were carefully transferred and spread on a sample holder. The crystals were investigated by a Bruker D4 Endeavor diffractometer (Karlsruhe, Germany) by using CuKα radiation λ=1.5406 Å radiation. The pattern were recorded in the range of 2θ=2-60 ° with a step size of 0.01 ° per step and with an acquisition time of 2s per step. During the measurement, a rotation speed of 30 rpm was added. A Bruker D8 ADAVANCE diffractometer (Karlsruhe, Germany) by using CuKα radiation λ=1.5406 Å radiation was also used to perform the XRPD measurement. In this case, the pattern were recorded in the range of 2θ=5-60 ° with a step size of 0.0074 ° per step.
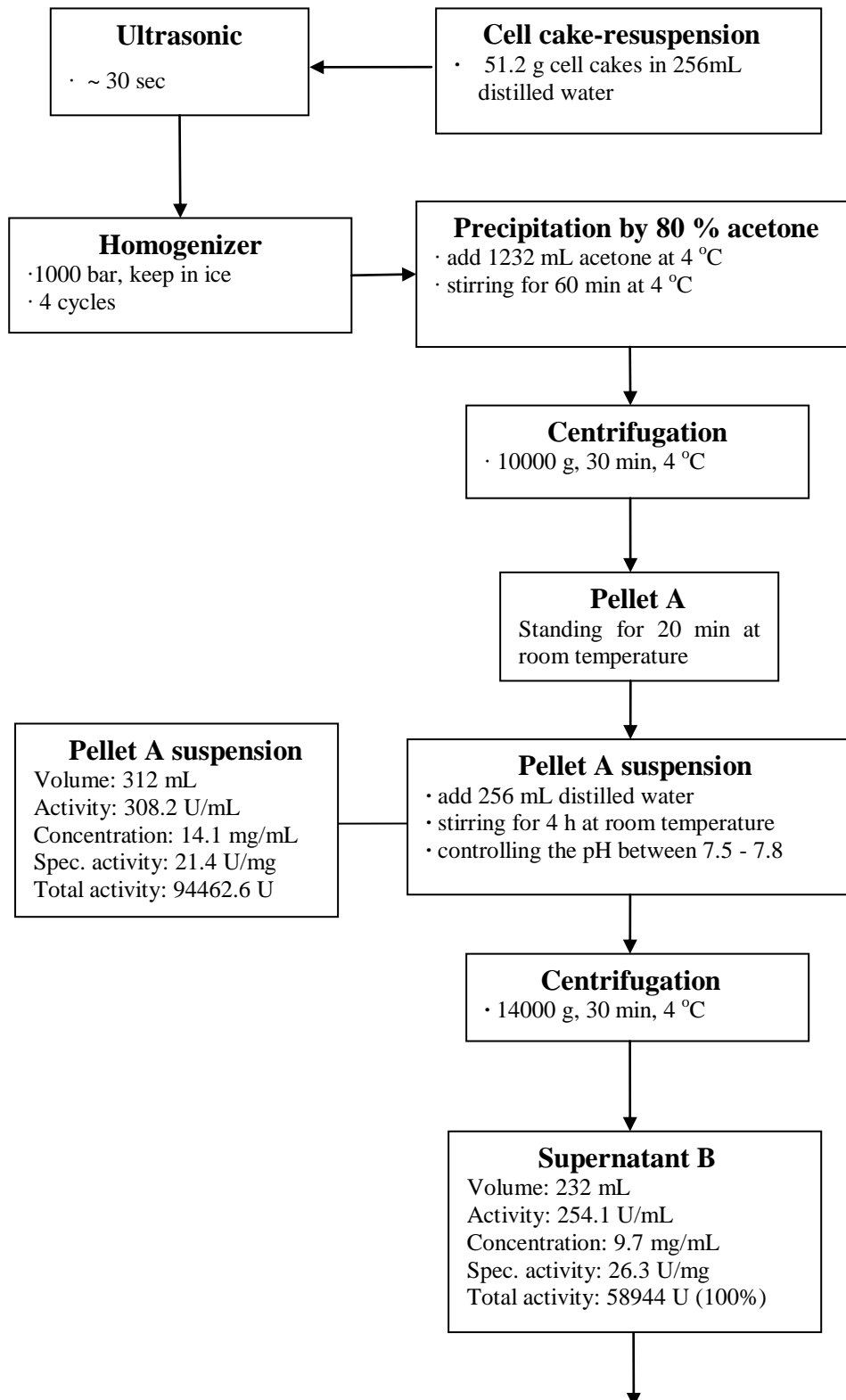
4. RESULTS AND DISCUSSION

4.1 L-asparaginase II Extract by Acetone Precipitation

The crude L-asparaginase II was obtained by twice acetone precipitation. Different from inorganic crystals, besides purity and crystallinity, the activity is essential for an enzymatic protein. A huge loss in activity during purification leads to an enzymatic protein to be worthless in further pharmaceutical application. Hence, L-asparaginase II samples were analyzed with an activity test over the whole time of procedure again and again. The activity values as well as the yield of total activities in series purification steps are illustrated in Figure 4.1-1. The purity of L-asparaginase II is represented in terms of specific activity. The specific activity of a protein is obtained from calculating the total activity present in solution divided by the total amount of protein present [Mc99]. The higher the specific activity reveals the higher purity of the interested protein in the solution. It is obvious that the specific activity of L-asparaginase II increases (from 21.4 U/mg in pellet A suspension to 35.7 U/mg in final extract) with the decrease of protein concentration (from 12.1 mg/mL in pellet A suspension to 4.1 mg/mL in final extract) in the solution. This result demonstrates that in the process of purification, the minor proteins in the sample solution were positively removed by the acetone precipitation. The decline of protein concentration after each purification step demonstrates that the contaminating proteins were effectively removed. This result is also supported by the estimation of SDS-PAGE (see Figure 4.1-2). As shown in Figure 4.1-2, the band with respect to L-asparaginase II is located at Mw=35kDa (outlined by arrow in Figure 4.1-2). The clear bands regarding minor proteins which are located in lane 2 reveals that the extract of L-asparaginase II obtained from the twice acetone precipitation still comprises many contaminating proteins. But the less in number of bands with respect to minor proteins existing in lane 3 of the solution of L-asparaginase II in an initial 50 mM tris-acetate buffer at pH 5.1 indicates that the purity of L-asparaginase II has been enriched.

Of course, it is noted that there is a loss of L-asparaginase II in each step. The final yield of the total activity of L-asparaginase II is less than the total activity present in the crude extract. If the total activity value after the 1st acetone precipitation was considered as 100%, after fractionation by tris-acetate buffer pH 5.1, the yield of total

activity of L-asparaginase II was 62.3%. This yield value was varied over the ranging from 55.6% to 62.3% in different batch of cell disintegration process.

Ultrasonic
· ~ 30 sec

Cell cake-resuspension
· 51.2 g cell cakes in 256mL distilled water

Homogenizer
·1000 bar, keep in ice
· 4 cycles

Precipitation by 80 % acetone
· add 1232 mL acetone at 4 ^{o}C
· stirring for 60 min at 4 ^{o}C

Centrifugation
· 10000 g, 30 min, 4 ^{o}C

Pellet A
Standing for 20 min at room temperature

Pellet A suspension
Volume: 312 mL
Activity: 308.2 U/mL
Concentration: 14.1 mg/mL
Spec. activity: 21.4 U/mg
Total activity: 94462.6 U

Pellet A suspension
· add 256 mL distilled water
· stirring for 4 h at room temperature
· controlling the pH between 7.5 - 7.8

Centrifugation
· 14000 g, 30 min, 4 ^{o}C

Supernatant B
Volume: 232 mL
Activity: 254.1 U/mL
Concentration: 9.7 mg/mL
Spec. activity: 26.3 U/mg
Total activity: 58944 U (100%)

Figure 4.1-1: Process diagram of one example of L-asparaginase II extract from cell disintegration
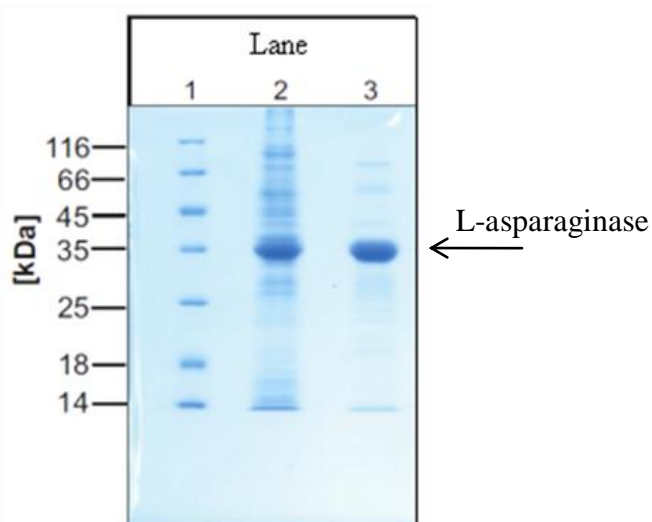
Figure 4.1-2: Commassie blue stained SDS-PAGE: Lane 1, molecular weight marker; Lane 2, extract of L-asparaginase II after a two times acetone precipitation; Lane 3, L-asparaginase II solution after tris-acetate buffer at pH 5.1 fractionation

Differences of specific activities of L-asparaginase II obtained between this work and previous works have been found. Table 4.1-1 gives the specific activities of L-asparaginase II reported in earlier works, obtaining from different purification methods.

In the previous works listed in Table 4.1-1, activity assays were all carried out by the Nesslerization method by measuring the absorbance regarding the amount of released ammonia, but, with a different pH value and at different wavelengths. In the present work, 50 mM Tris-HCl buffer at pH 8.6 was added to carry out hydrolysis reaction and the released ammonia was calculated by reading the absorbance at 436 nm (see **Chapter 3.2.2**). The different conditions of hydrolysis media and the absorbance value read at different wavelength are the reasons of obtaining different specific activity.

Table 4.1-1: Summaries of specific activity of L-asparaginase II prior to crystallization in some earlier works

Previous Work	Source of Biomass	Purification Steps	Wavelength of ammonia determination [nm]	pH values	Specific Activity [U/mg]
Rauenbusch et al. [Rau70]	*E.coli* ATCC 9637	- two times acetone precipitate	540	7.2	18 (one unit based on 1 min)
Ho et al. [Ho70]	*E.coli* B ATCC 13706	- pH 4.5 extract - $(NH_4)_2SO_4$ precipitate - dialysis - ethanol precipitate	480	8.6	60 (one unit based on 1min)
Wagner et al. [Wag73]	*E.coli* ATCC 9637	- two times acetone precipitate - pH 8.5 extract	Not mentioned	8.5	300 (one unit based on 30 minutes)
Roberts et al. [Rob68]	*E.coli* HAP	- ethyl alcohol fractionation - EDTA-cellulose chromatography and concentration - CM-Sephadex chromatography and concentration - Polyacrylamide electhophoresis and concentration	Not mentioned	8.0	620 (one unit based on 1 min)
Whelan and Wriston [Whe69]	*E.coli* B	- $MnCl_2$ heat - P-150 Bio-Gel - DEAE-cellulose - Calcium hydroxylapatite - Pre-disc electrophoresis	500	8.5	400 (one unit based on 1 min)
Boyd and Phillips [Boy71]	Serratia marcescens ATCC60	- Heat; $MnCl_2$ - KOH; freeze-thaw - DEAE cellulose chromatography - $(NH_4)_2SO_4$ fractionation - Hydroxylapatite chromatography - Polyacrylamide gel electrophoresis	500	7.4	255 (one unit based on 1 min)
Nakamura et al. [Nak71]	*E.coli* A-1-3 KY3598	- homogenate - two times ethanol fractionation - acid treatment - DEAE Chromatography - CM Sephadex Chromatography	Not mentioned	8.0	195 (one unit based on 1 min)

Another reason causing the varied specific activity might be the different purification process. It is found that the specific activity of L-asparaginase II after no more than two purification steps by organic solvent fractionation (e.g. acetone or ethanol) is only falling within the range of 10-18 U/mg. Ho et al. [Ho70] reported a value of 60 U/mg after four purification steps. Other specific values up to 620 U/mg prior to the crystallization steps reported by Roberts et al. [Rob68], without exception, were obtained by chromatography. There is no denying that chromatography is high selective and wide employed in protein purification. However, in the present work, a much simpler, more efficient purification method is preferred, if crystals can be obtained successfully.

4.2 Determination of Phase Diagrams of L-asparaginase II
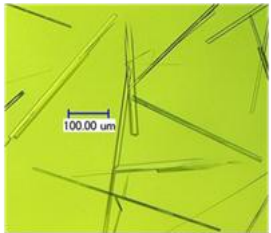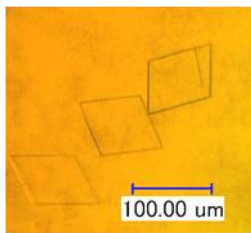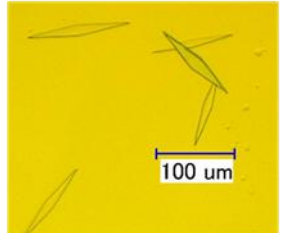
4.2.1 Screening Trails of Crystallization in Solution

Wagner et al. [Wag69] suggested that only the asparaginase with a specific activity of more than 180 U/mg can be crystallized by PEG at its pI. However, Ho et al. [Ho70] obtained crystalline asparaginase successfully by the addition of ethanol in an initial asparaginase having specific activity of 71 U/mg at pH 6.6 to 6.7. In the present work, by experiments trials, the initial L-asparaginase II solution (after two times acetone precipitation and pH 5.1 extract) having a specific activity ranging from 26.9 U/mg to 35.7 U/mg were suitable for crystallization in solution supplemented with PEG_{6000}, ethanol and MPD in an initial 50 mM tris-acetate buffer solution at pH 5.1.

The primary screening tests of crystallization were carried out by the method of crystallization in solution supplemented with PEG_{6000}, ethanol and MPD. The complete crystallizations were executing in a 96-well microplate at a constant temperature of 8 ℃. However, concerning supplemented with PEG_{6000}, a room temperature was enough to achieve the crystalline L-asparaginase II.

The example of crystal shapes of L-asparaginase II formed with a certain precipitant agents was given in Table 4.2-1.

Table 4.2-1: Crystalline L-asparaginase II formed in different precipitant agents

Initial Protein concentrations	1.4 - 4.1 mg/mL		
Buffer solution	50 mM (initial concentration) Tris-acetate pH 5.1		
Precipitant agents	PEG$_{6000}$	cold ethanol	cold MPD
Further treatment	Insoluble particles were removed by centrifugation after adding a certain precipitant agent, and transfer the solution to a microplate		
Temperatures and days	RT, overnight	8°C, 7 days	8°C, 14 days
Crystals shape	Rod-shape	Rhombus-shape	Prism-shape

In order to ensure that the crystals formed in the different precipitant agents are really crystalline L-asparaginase II, SDS-PAGE tests were performed. The results of the SDS-PAGE are given in Figure 4.2-1 and the bands with respect to L-asparaginase II in two gels are located at the molecular weight of 35 kDa. The sharp bands, which are due to L-asparaginase II in lane 4 (in Figure 4.2-1a) locating the sample of the dissolved crystals formed with PEG$_{6000}$, in lane 6 (in Figure 4.2-1a) locating the sample of the dissolved crystals formed with ethanol and in lane 5 (in Figure 4.2-1b) locating the sample of the dissolved crystals formed with MPD, make sure that the crystals derive from L-asparaginase II.
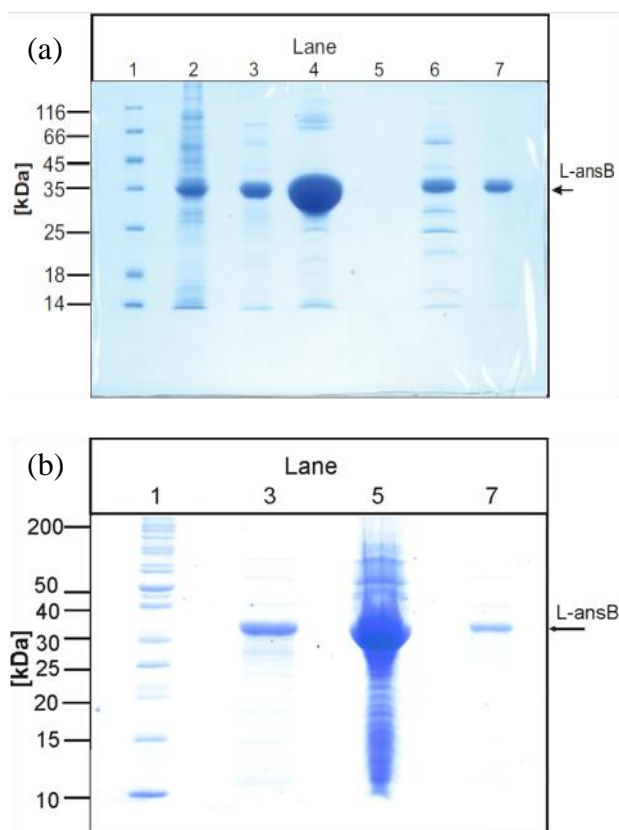
Figure 4.2-1: SDS-PAGE stained by Coomassie brilliant blue. **(a):** Lane 1, molecular weight marker; Lane 2, crude extract of L-asparaginase II after twice acetone fractionation; Lane 3, pH 5.1 extract of L-asparaginase II solution; Lane 4, dissolved crystals induced by PEG_{6000}; Lane 5, mother liquor of crystals induced by PEG_{6000}; Lane 6, dissolved crystals induced by ethanol; Lane 7, mother liquor of crystals induced by ethanol. **(b):** Lane 1, molecular weight marker; Lane 3, pH 5.1 extract of L-asparaginase II solution; Lane 5, dissolved crystals induced by MPD; Lane 7, mother liquor of crystals induced by MPD

It should be noted, however, that minor bands exist owing to contaminating proteins in that samples obtained from the two times acetone precipitation. However, those minor bands, by comparison, are much weaker than the sharp bands of L-asparaginase II. One reason for the existence of such contaminating proteins in the dissolved crystals samples may be caused by the solid particles of contaminating proteins accompanied with crystals when they were separated from the mother liquor by filter centrifuge. As shown in Figure 4.2-2, it is visible that many small solid particles occupy the background of the crystallization well under the digital microscope. It has been introduced that the pore size of the membrane of the centrifugal filter unit is

0.45 μm (see Table 3.1-3), thus, it is difficult to separate crystals from mother liquor without the solid particles.
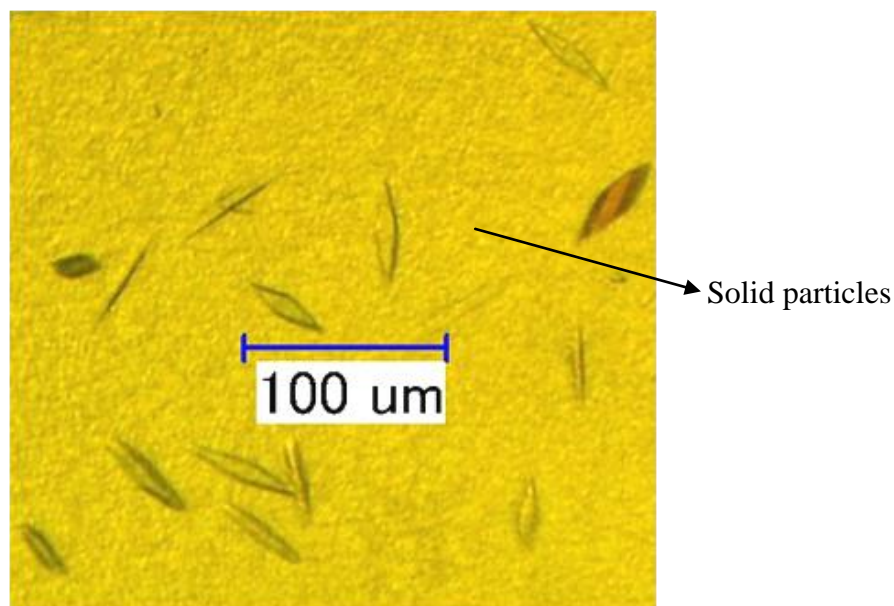
Figure 4.2-2: Prism-shape crystals of L-asparaginase II

SDS-PAGE results show that the crystals, formed in the presence of PEG_{6000}, ethanol and MPD, respectively, consist of L-asparaginase II as expected. It demonstrates that the pH 5.1 extract of L-asparaginase II obtained from twice acetone precipitation in the present work can be crystallized successfully by adding a given precipitant agent, even though their specific activities are smaller than those values reported in other works. That is crucial for the followed determination of the phase diagram.

4.2.2 Phase Diagram for Crystallization of L-asparaginase II including MZW

Based on the trials, the phase diagrams of L-asparaginase II including MZW in the presence of PEG_{6000}, ethanol and MPD in given conditions were established by using an online turbidity technique, respectively. These phase diagrams are illustrated in Figures 4.2-3, 4.2-4 and 4.2-5. Notably, besides the phase diagrams plotting protein concentration as a function of temperature (see Figures 4.2-3a, 4.2-4a and 4.2-5a), another type of phase diagrams plotting enzymatic activity versus temperature was introduced, too (see Figures 4.2-3b, 4.2-4b and 4.2-5b).

The phase diagrams plotting enzymatic activity as a function of temperature were introduced in the present work for the first time. In previous studies, most proteins for

the phase diagram determination were purchased from a company (see <u>Table 4.2-2</u>) and were used without further purification since no other contaminating proteins were supposed to exist in these commercial products. Therefore, the phase diagrams established in their works were certainly those of the protein of interest. On the contrary, the protein samples in the present study derive from a recombinant *Escherichia coli* cultivated in the lab (see Figure 4.1-1). In the SDS-PAGE, other contaminating proteins were detected in the L-asparaginase II solution extracted from the biomass. It is therefore necessary to make sure that the crystallization behavior is dominated by L-asparaginase II.

As mentioned above, all protein concentrations of the sample solution were estimated by an assay according to the method described by Bradford et al. [Bra76]. This method relies on monitoring the increase in the absorption at 595 nm because of the binding of the dye Commassie Brilliant Blue G-250 to proteins (see **Chapter 3.2.2**). It is noted that the protein concentration values obtained from this method involves the total amount of all proteins, which means including all contaminating proteins and denatured or inactive forms of the protein itself. The catalytic activity of L-asparaginase II is the crucial property for the treatment of acute lymphatic leukemia (ALL). Finally, the activity is the most important parameter in the purification of L-asparaginase II including the crystallization and is more precise to characterize the protein of interest as an enzyme than the protein concentration.

Table 4.2-2: The sources of proteins for phase diagram determination in previous studies

Previous researches	Protein of interest	Sources
Pusey and Gernert [Pus88]	Hen's egg white lysozyme	grade 1, lot # 65F8171, Sigma Chemical Co.
Cacioppo et al. [Cac91]	Hen's egg white lysozyme	grade III, Sigma Chemical Co.
Muschol and Rosenberger [Mus97]	Hen's egg white lysozyme	Seikagaku America, lots E94203 and E94Z05
Lin et al. [Lin08]	lysozyme (chicken egg white) catalase (bovine liver) ribonuclease A (type II bovine pancreas) ribonuclease S (bovine pancreas) trypsin (bovine pancreas) concanavalin A (cancanvalin ensiformis) papain (papaza latex) proteinase K (tritirachium album) chymotrypsinogen A (bovine) ELP16 (Rattus norvegicus)	Sigma / Aldrich
Aldabaibeh et al. [Ald09]	Hen's egg white lysozyme	Fluka
Liu et al. [Liu10]	Hen's egg white lysozyme	Sigma-Aldrich, Singapore
Maosoongnern et al. [Mao12]	Hen's egg white lysozyme	Fluka
Ryu and Ulrich [Ryu12]	Hen's egg white lysozyme	Fluka, product no. 62971
Müller [Mül12]	Hen's egg white lysozyme	Fluka

The activity value is expressed as an enzyme unit, i.e. U, where 1U reveals the amount of enzyme that catalyzes the formation of 1 μmol of ammonia in 1 minute [Ho70]. The released ammonia was calculated from the absorbance at 436nm. The samples used for the activity test (Nesslerization) derived from the same sample

solution for protein concentration assay. The advantage of using enzymatic activity of L-asparaginase II instead of protein concentration in the present work is that it is positive to eliminate the interference of other contaminating proteins and inactive forms of target protein in the phase diagram. Moreover, phase diagrams for crystallization behaviour of L-asparaginase II which are established on the basis of crude materials are applicable in industrial production when crystallization is utilized as a mild purification technique.

Good agreement regarding the crystallization behavior is obtained in all phase diagrams, no matter if plotting protein concentration versus temperature or plotting enzymatic activity versus temperature. Over the range of conditions investigated in the present work, the solubility of crystalline L-asparaginase II crystals has an upward trend with an increase of temperature. The spontaneous nucleation of L-asparaginase II in one certain precipitant agent occurs at a higher temperature when the concentration of L-asparaginase II is higher.

It should be noted that in Figure 4.2-3 the nucleation data of L-asparaginase II in the presence of PEG_{6000} are less in number than those of the solubility data. This is due to the difficulty in grasping the exactly nucleation point simultaneously in one cycle of online measurement while the sample solution supplemented with PEG_{6000}. The valid nucleation temperature was adopted only when at which the IR-reading signal (transmission) started to decrease in the cooling process. When the sample solution contains a high protein concentration or contains a high PEG_{6000} concentration the nucleation might begin as soon as PEG_{6000} had been added to the initial protein solution. Because it existed a delay of approximate 30-60 min before starting of recording program.
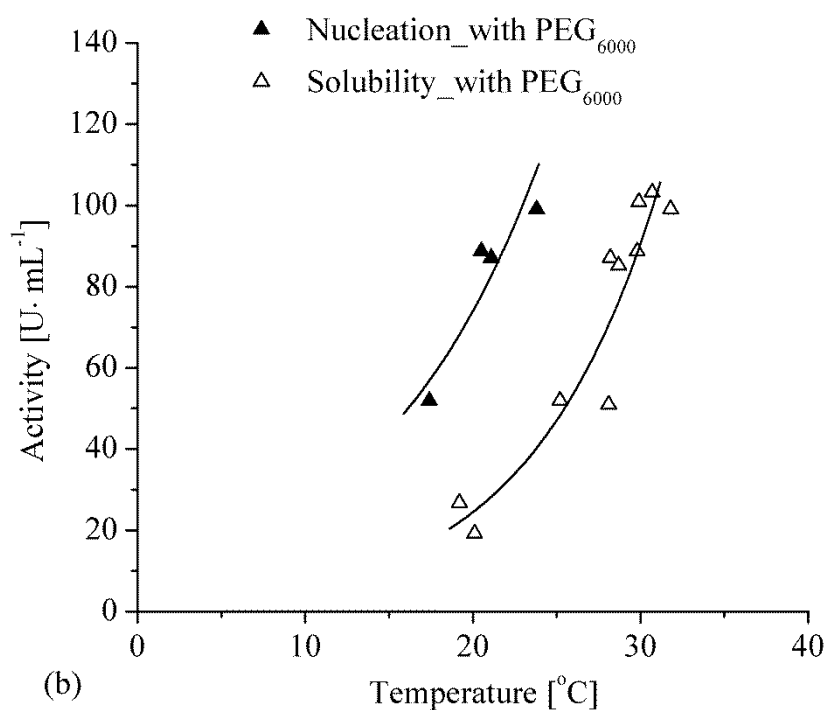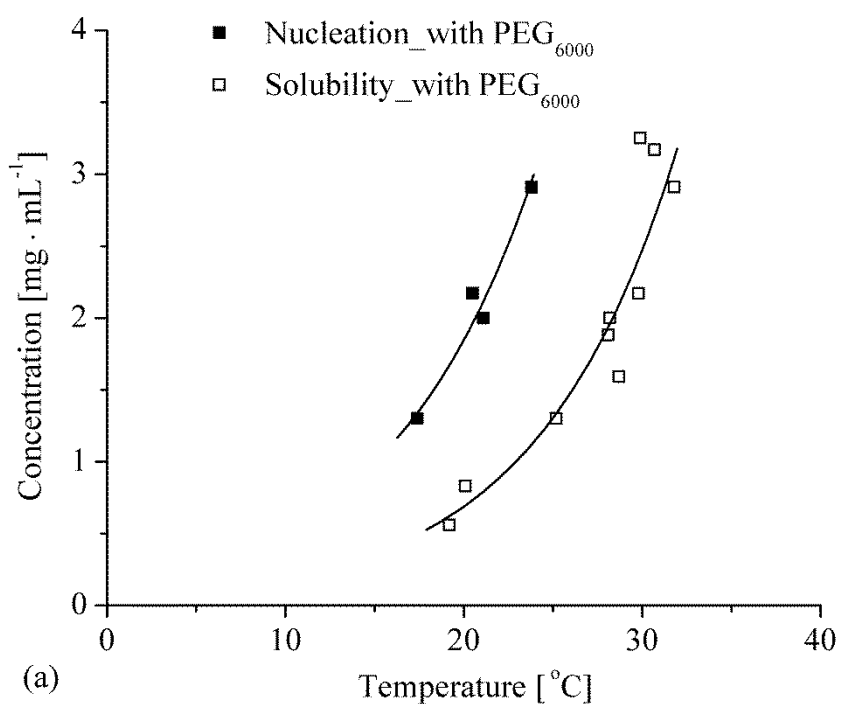
Figure 4.2-3: Phase diagrams of L-asparginase II including MZW in the presence of 4.1-8.3% (w/v) PEG$_{6000}$, in 50 mM (initial concentration) tris-acetate buffer pH 5.1. (a): plotting concentration versus temperature (b): plotting enzymatic activity of L-asparaginase II versus temperature
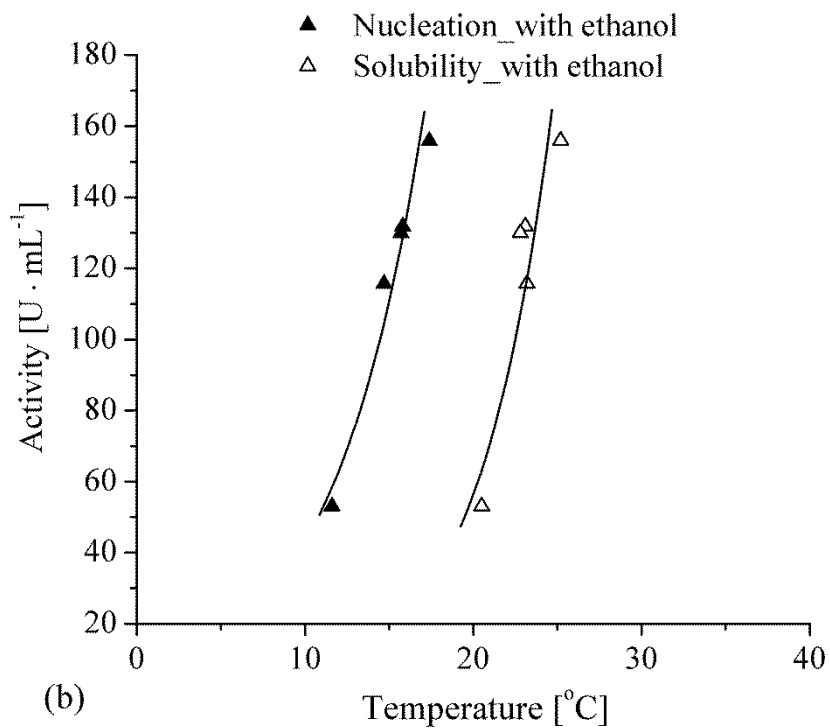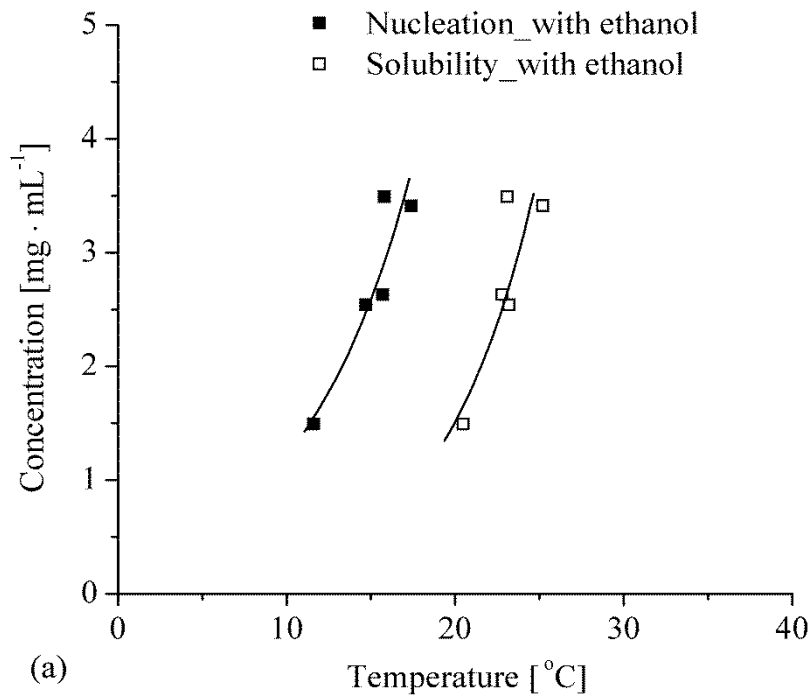
Figure 4.2-4: Phase diagrams of L-asparginase II including MZW in the presence of 13.0-28.6% (v/v) ethanol, in initial 50 mM tris-acetate buffer pH 5.1. (a): plotting concentration versus temperature; (b): plotting enzymatic activity of L-asparaginase II versus temperature

Figure 4.2-5: Phase diagrams of L-asparginase II including MZW in the presence of 15.3-22.8% (v/v) and in the presence of 28.6% (v/v) MPD, respectively, in initial 50 mM tris-acetate buffer pH 5.1. (a): plotting concentration versus temperature; (b): plotting enzymatic activity of L-asparaginase II versus temperature
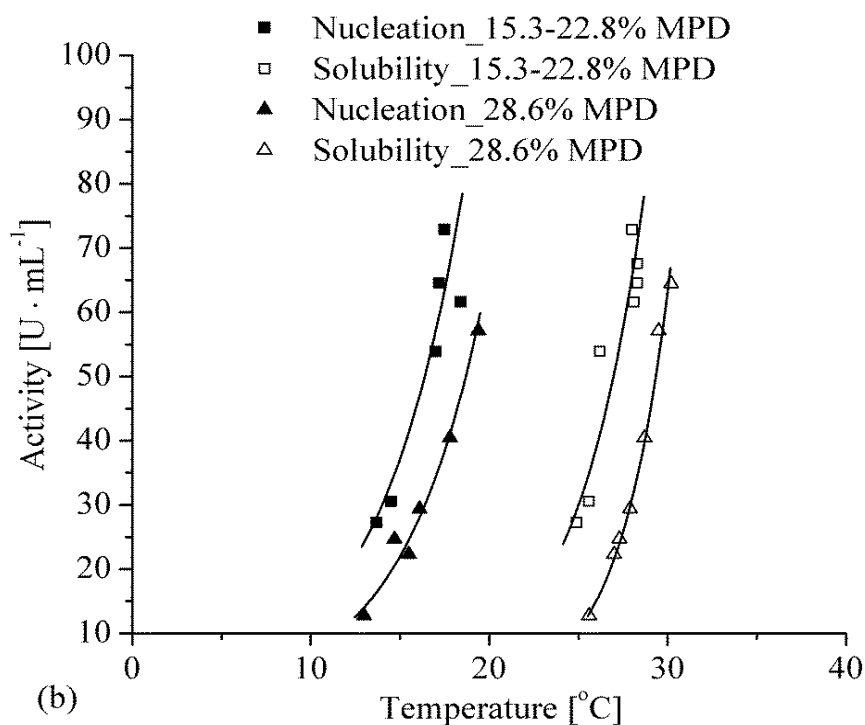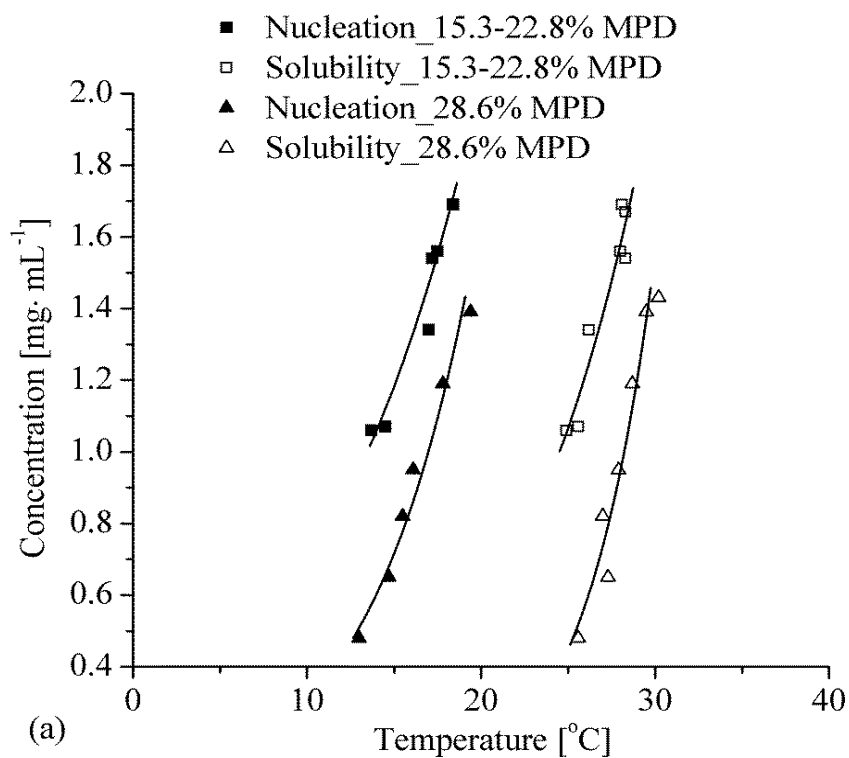
The metastable zone width (MZW) is defined as the distance between nucleation and solubility with respect to temperature at the same level of protein concentration. The MZW is one of the most important parameters for design and control of an industrial crystallization. Theoretically, the optimal condition for crystal growth in an industrial crystallizer is in the middle of the MZW [Hof13]. It is much easier to control the optimal condition of crystal growth when there is a broader metastable zone. The phase diagrams, i.e. Figures 4.2-3, 4.2-4 and 4.2-5, indicate that the MZW of the phase diagram with ethanol (~10 ℃) and the MZW of the phase diagram with MPD (~10-11 ℃)are broader than that with PEG$_{6000}$ (~8 ℃) under the given conditions in the present study. This result shows that the spontaneous nucleation of L-asparaginase II in the presence of ethanol as well as in the presence of MPD requires a lower temperature than that in the presence of PEG$_{6000}$.

 Compared with the phase diagrams of lysozyme including the MZW in the presence of NaCl reported by Maosoongnern et al. [Mao12], a good agreement is obtained between L-asparaginase II and lysozyme. The solubility of these two kinds of crystals increases with an increase in temperature, and the spontaneous nucleation increases at a higher temperature when the protein concentration is higher. However, lysozyme possesses a broader MZW of 25 ℃ in the presence of NaCl at pH 5.0, while L-asparaginase II has a maximum MZW of 11 ℃ in the presence of MPD. But it is notable that Maosoongnern et al. [Mao12] applied a lower agitating speed of 350 rpm during the measurement of lysozyme phase diagram. Here, an agitating speed of 500 rpm-1000 rpm was used. The increase of agitating speed would narrow the MZW [Mul01].

 The influence of the increasing amount of MPD was studied by determining the nucleation and solubility temperatures of sample solutions contained varied protein concentrations but at a constant MPD concentration of 28.6% (v/v). The nucleation and solubility data collected in the presence of 28.6% (v/v) MPD are illustrated in Figure 4.2-5. They are graphed together with those curves regarding the crystallization behaviour at a lower MPD concentration ranging 15.3-22.8% (v/v). By comparison, it can be observed that the nucleation and solubility data of L-asparaginase II concurrently shift to a higher temperature area with the rise in concentration of MPD. This phenomenon demonstrates that increasing MPD concentration will result in arriving ahead at spontaneous nucleation and reducing the solubility of L-asparaginase II. The same conclusion was also reported by Ries-Kautt

and Ducruix [Rie89] as well as Maosoongnern et al. [Mao12] in their case study of lysozyme with various salt concentrations.

There is a small increase by ~1 ℃ of MZW with MPD concentration, which is contrary to that result reported by Maosoongnern et al. [Mao12], who represented that at the protein concentration of 40 mg/mL the MZW expressed in temperatures decreased with an increasing in NaCl concentrations from 3% to 5% at pH 4.4, pH 5.0 and pH 6.0. However, in the present work, L-asparaginase II solution with concentration smaller than 2.0 mg/mL was studied.

Compared to the curves regarding the samples contained a constant MPD concentration of 28.6% (v/v), the nucleation and solubility curves of the samples at a MPD concentration ranging 15.3-22.8% (v/v) appear not to be different in their upward trend (see Figures 4.2-5a, b). This phenomenon also occurs in the solubility curves of tetragonal lysoyzme crystals at a given pH value with different concentrations of sodium chloride, which reported by Forsythe et al. [For99]. The solubility data collected at pH 5.0 and at pH 5.2 reported by Forsythe et al. [For99] are graphed here in <u>Figure 4.2-6</u>, respectively, over the same range of conditions as those investigated in the present work (i.e., protein concentration is below 2.0 mg/mL, temperature scale is from 0 to 40°C). In Figure 4.2-6, the solubility of lysozyme crystals decreases with increasing salt concentration. However, at pH 5.0, the solubility data partly overlap in the presence of 5% NaCl and 7% NaCl (see Figure 4.2-6a). At pH 5.2, this partly overlap phenomenon occurs in the presence of 4% NaCl and 5% NaCl, and solubility data separate again when the NaCl concentration is 7% (see Figure 4.2-6b). Therefore, it could be understood that the solubility data of crystalline L-asparaginase II collected in the present condition might partly overlap within the MPD concentration of 15.3-22.8% (v/v). When the MPD concentration increases to 28.6%, the solubility curve of crystalline L-asparaginase II separates from those curves regarding the samples at lower MPD concentrations, but without changes on the upward trend. The same phenomenon of data partly overlapping might also exists in the nucleation and solubility curves regarding the crystallization solutions supplemented with PEG$_{6000}$ ranging 4.1-8.3% (w/v) as well as those regarding the solutions supplemented with ethanol ranging 13.0-28.6% (v/v).
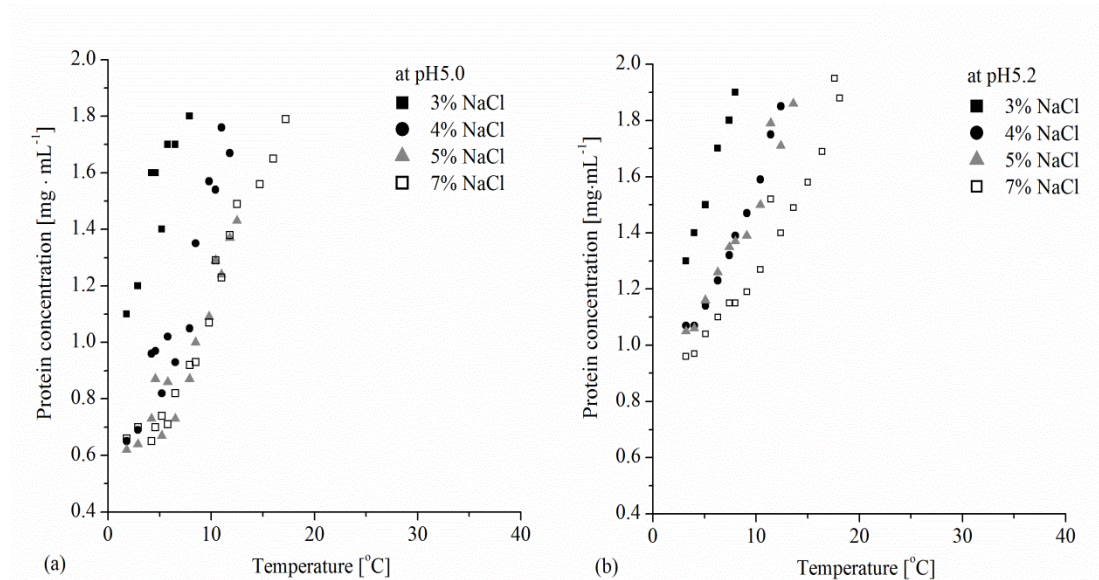
Figure 4.2-6: Solubility curves with temperature of lysozyme crystals in different concentrations of sodium chloride reported by Forsythe et al. [For99] (a): solubility curves at pH 5.0; (b): solubility curves at pH 5.2

On the other hand, the solubility values of lysozyme reported by other investigators result from commercial products which possess higher purity of the target protein (as shown in Table 4.2-2). On the contrary, the L-asparaginase II sample applied in the present work was extracted from frozen recombinant *Escherichia coli* cells as described previously [Liu13]. As mentioned above, the protein concentration determined by a Bradford assay [Bra76] applied in the present work comprises the total amount of all proteins, i.e., including the contaminating proteins and denatured or inactive forms of the target protein. Therefore, the phase diagram plotting enzymatic activity of L-asparaginase II versus temperature (as shown in Figures 4.2-3b, 4.2-4b and 4.2-5b) introduced in this paper is necessary, in order to eliminate the influences from contaminating proteins on crystallization behavior. The nucleation and solubility curves plotting in different parameters show the same crystallization behavior, which demonstrates that the nucleation and solubility data collected in the present work show positively the success of the approach for the active L-asparaginase II.

The outstanding advantage of establishing the phase diagram for crystallization plotting enzymatic activity of L-asparaginase II versus temperature is that it is possible to provide information guiding the crystal growth of L-asparaginase II in a

multi-component system, when the crystallization as a technology serves as a purification and separation method in industrial application.

4.3 Solubility and Crystal Modifications

If the solubility curves obtained in recent work, i.e. one with PEG_{6000}, one with ethanol and the third with MPD are plotted in one graph together, it is obvious that they do not overlap as well as not increase with the same slope, regardless whether the curves are expressed in terms of protein concentration versus temperature (Figure 4.3-1a) or in terms of enzymatic activity versus temperature (Figure 4.3-1b). The microscope images of those crystals displaying respectively in Figures 4.3-1c, 4.3-1d and 4.3-1e, the crystal forms are not identical when different precipitant agents are applied. Figure 4.3-1c shows the rectangular crystals formed with 8.3% (w/v) PEG_{6000}, Figure 4.3-1d represents the image of rhombic crystals resulting from the present of 23.0% (v/v) ethanol, and the image of plasmatic crystals formed in the presence of 28.6% (v/v) MPD is illustrated in Figure 4.3-1e.

Up to date, it is not very clear in classical theory whether there could be two crystal modifications when different precipitants are used [Bec00][Bec13]. However, the solubility of crystals in a certain solvent with respect to the crystal forms can be understood according to the explanation from Hilfiker [Hil13]. Hilfiker suggests that the solubility of form X of a substance A is defined as the state where the free energy of the solid (G_{solid} (A^X)) is equal to the free energy of the solution ($G_{solution}$ $(A)^X$), which is shown in Equation 4.3-1.

$$G_{solid}\ (A^X) = G_{solution}\ (A)^X \tag{4.3-1}$$

Considering the activity of the solid is 1, the Equation 4.3-2 can be obtained.

$$G^0_{solid}\ (A^X) = G^0_{solution}\ (A) + RT\ ln\ a[A]_X \tag{4.3-2}$$

Here G^0_{solid} (A^X) and $G^0_{solution}$ (A) represent the standard free energy of A in the solid state and A in the solution state, respectively. $a[A]_X$ is the activity of A as form X in the solution. The activity of A in the solution can be expressed in Equation 4.3-3.

$$\mathbf{a[A] = f(A) \times c[A]} \hspace{4cm} \text{(4.3-3)}$$

f(A) is the activity coefficient and c[A] is the concentration of a saturated solution of A. f(A) is approximately 1 when the solubility of A in a solvent is assuming very small, so that c[A] can be substituted for a[A] (as shown in <u>Equation 4.3-4</u>).

$$\mathbf{G^0_{solid} (A^X) \approx G^0_{solution} (A) + RT \ln c[A]_X} \hspace{2cm} \text{(4.3-4)}$$

To sum up, the free energy differences of form I and form II of substance A in a given solvent can be calculated by <u>Equation 4.3-5</u> through measuring the solubility of different forms in solution, respectively.

$$\mathbf{G^0_{solid} (A^I) - G^0_{solid} (A^{II}) \approx RT \ln \{c[A]_I / c[A]_{II}\}} \hspace{1.5cm} \text{(4.3-5)}$$

For this reason, it can be understand that if assuming that the active coefficient of A in the solvents is close to 1 (i.e. the solubility of A in the solvent is small), at the same temperature the higher standard free energy of solid A in form I results in a higher solubility of form I of substance A. This means form I of A is more unstable than form II of substance A and thus the solubility curve of form I should be located higher than that corresponding form II, if expressing in terms of a phase diagram plotting concentration versus temperature.

Return to the solubility curves in Figures 4.3-1a, b, it is evident that the locations of the solubility curves of crystalline L-asparaginase II corresponding with ethanol, PEG$_{6000}$ and MPD are in the order from highest to lowest, respectively, over the range of conditions studied. This phenomenon reveals that the prism-shape crystals of L-asparaginase II with MPD concentration of 28.6% (v/v) are the most stable, while the rhombus-shape crystals of L-asparaginase II in the presence of ethanol at a concentration ranging 13.0-28.6% (v/v) are the most unstable. This occurrence is corresponding with the following results of X-ray diffraction (see **Chapter 4.4**).

(a)

(b)
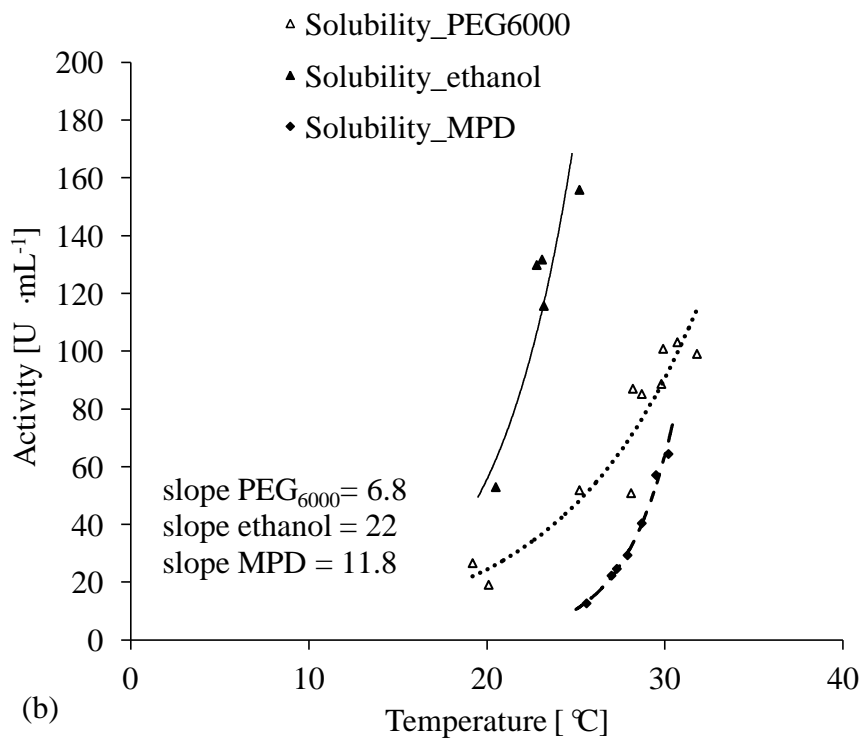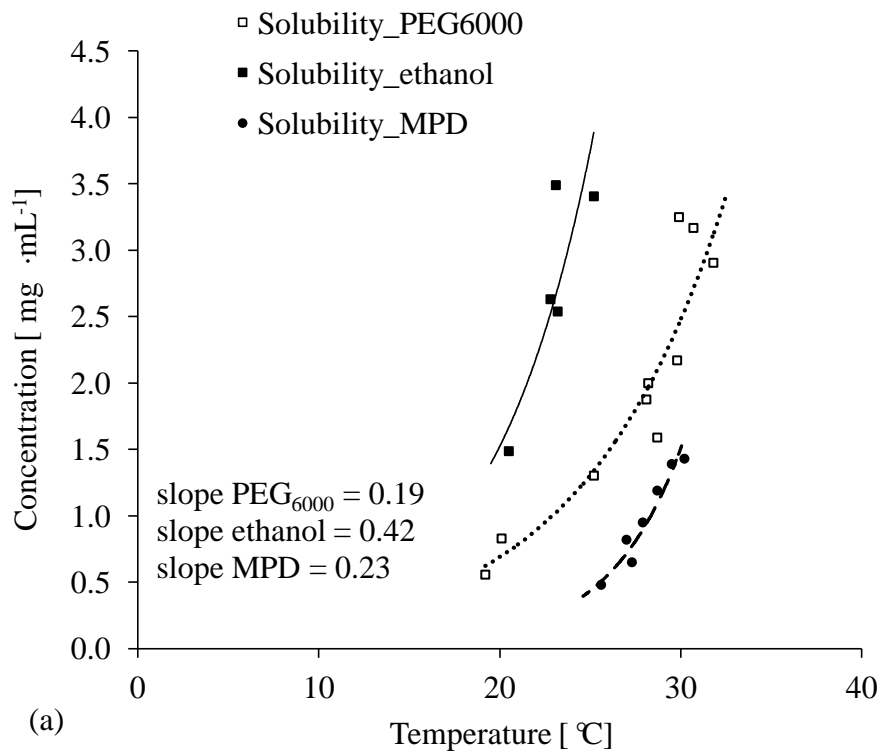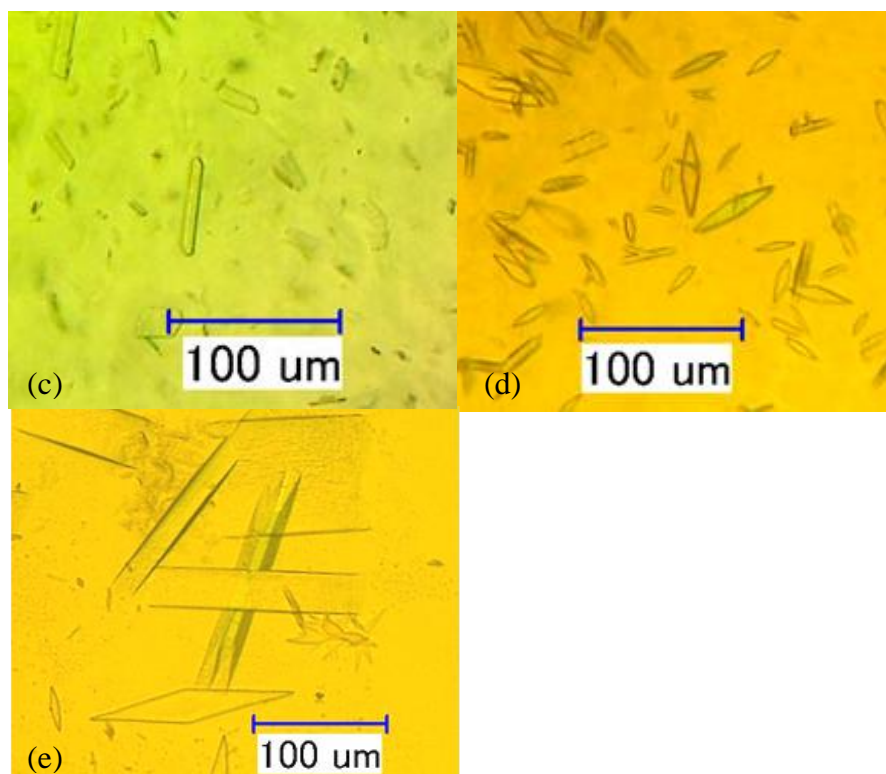
Figure 4.3-1: Solubility curves of L-asparaginase II in the presence of 4.1-8.3% (w/v) PEG$_{6000}$, 13.0-28.6% (v/v) ethanol, 28.6% (v/v) MPD and the microscope images of crystalline L-asparaginase II in the three precipitant agents, respectively, in 50 mM (initial concentration) Tris-acetate buffer pH 5.1. (a): solubility curves plotting <u>protein concentration versus temperature</u>; (b): solubility curves plotting <u>enzymatic activity versus temperature</u>; (c): rectangular shaped crystals formed in the presence of 8.3% (w/v) PEG$_{6000}$; (d): rhombic shaped crystals formed in the presence of 23% (v/v) ethanol; (e): prismatic shaped crystals formed in the presence of 28.6% (v/v) MPD

4.4 Crystal Structure Analyzed by X-ray Diffraction

4.4.1 Single crystal X-ray diffraction

In order to identify the internal structure of the crystals formed with different precipitant agents, the crystals obtained from the crystallization experiments (see above) were investigated by X-ray diffraction analysis. The most precise technique to identify the atomic and molecular structure of a crystal is the single crystal X-ray diffraction, which can produce a 3-dimensional picture of the density of electrons within the crystal by calculating the angles and intensities of those diffracted pattern.

Single crystal X-ray diffraction data collected successfully from one prism-shaped crystal with the size of 0.1 mm $\times$ 0.1 mm $\times$ 0.06 mm (length of one side $\times$ length of another side $\times$ thickness, as shown in Figure 4.4-1), forming at 8 ℃ in the presence of 26% (v/v) MPD. Thin prism-shaped crystals firstly with size of 0.06 mm $\times$ 0.06 mm $\times$ 0.01 mm were visible under a microscope after 14 days, growing to the maximum dimensions until diffraction in the subsequent one month. The data sets were integrated by XDS [Kab10a, b] and scaled by SCALA [Eva06]. The prism-shaped crystals are orthorhombic and belong to the space group of $P2_12_12_1$ as determined by POINTLESS [Eva06] with the unit-cell parameters a=93.9, b=125.77, c=151.75Å. These values are quite similar to the results reported by Palm et al. [Pal96] (PDB code 4ECA). Both data-collection statistics were summarized in Table 4.4-1.
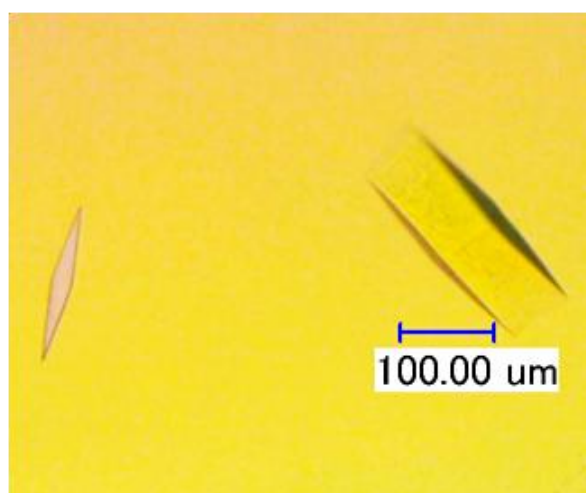
Figure 4.4-1: Microscope image of crystalline L-asparaginase II in the presence of 26% (v/v) MPD, in initial 50 mM tris-acetate buffer pH 5.1

The X-ray pattern obtained in the present work are not perfect isotropic, which means the crystal quality is not good when growing through the method of crystallization in solution (as expected). In protein crystallography, the value of R_{merge} (also known as R_{sym}) is commonly used to summarize the data quality [Kab10a]. The R_{merge} with values of < 0.05, 0.05-0.1, 0.1-0.2 and > 0.2 respectively indicate good, usable, marginal, and questionable quality data [Die97]. In the present work R_{merge}= 0.339 might be caused by the fact that single crystal under X-ray diffraction is of a twinning or mosaic crystal (see under described in Figure 4.4-3). Thus, it is failed to carry out further refinement of the structure.

Table 4.4-1: Summary of crystal graphic data and crystallization conditions

Values in the parenthesis are for the highest resolution shell

	Data from the present work	Data from Palm et al.[Pal96]
Space group	$P2_12_12_1$	$P2_12_12_1$
Unit-cell parameters		
a [Å]	93.9	95.0
b [Å]	125.77	126.2
c [Å]	151.75	155.7
Temperature [K]	100	103
Wavelength [Å]	1.5418	1.5418
Oscillation range [°]	0.5	0.5
Resolution [Å]	29.5-2.88	20.0-2.2
Unique reflections	41382	68197
Completeness [%]	99.9 (99.9)	72 (58)
R_{merge}	0.339 (0.930)	0.102 (0.41)
$\langle I/\sigma(I)\rangle$	5.4 (2.0)	11.0 (2.2)
Crystallization method	Crystallization in solution	Hanging-drop technique (vapor diffusion)
Protein concentration	2.0 mg/mL (initial solution)	17 mg/mL
Crystal dimensions [mm]	$0.1 \times 0.1 \times 0.06$	$0.5 \times 0.5 \times 0.15$
Solutions	50 mM (initial concentration) Tris-acetate pH 5.1 (protein buffer)	10 mM Tris-HCl, pH 7.0 (protein buffer)
	26% MPD	36% MPD, 100mM sodium aspartate, 100 mM sodium acetate, pH 5.0

It is known that a crystal is made up of repeating units and each unit cell possesses the same number of atoms [Abd07]. The unit cells can be characterized by a set of lengths a, b, and c (the shortest edges of a cell in three dimensions), and three angles α, β and γ (intersection angles between the edges) [Mye02]. The six numbers of lengths

and angles are so called unit cell parameters (or lattice parameters) of a single crystal. It is commonly agreed upon that there are 14 possible lattices distinguished by those six parameters and are known as Bravais lattices (see Figure 4.4-2).
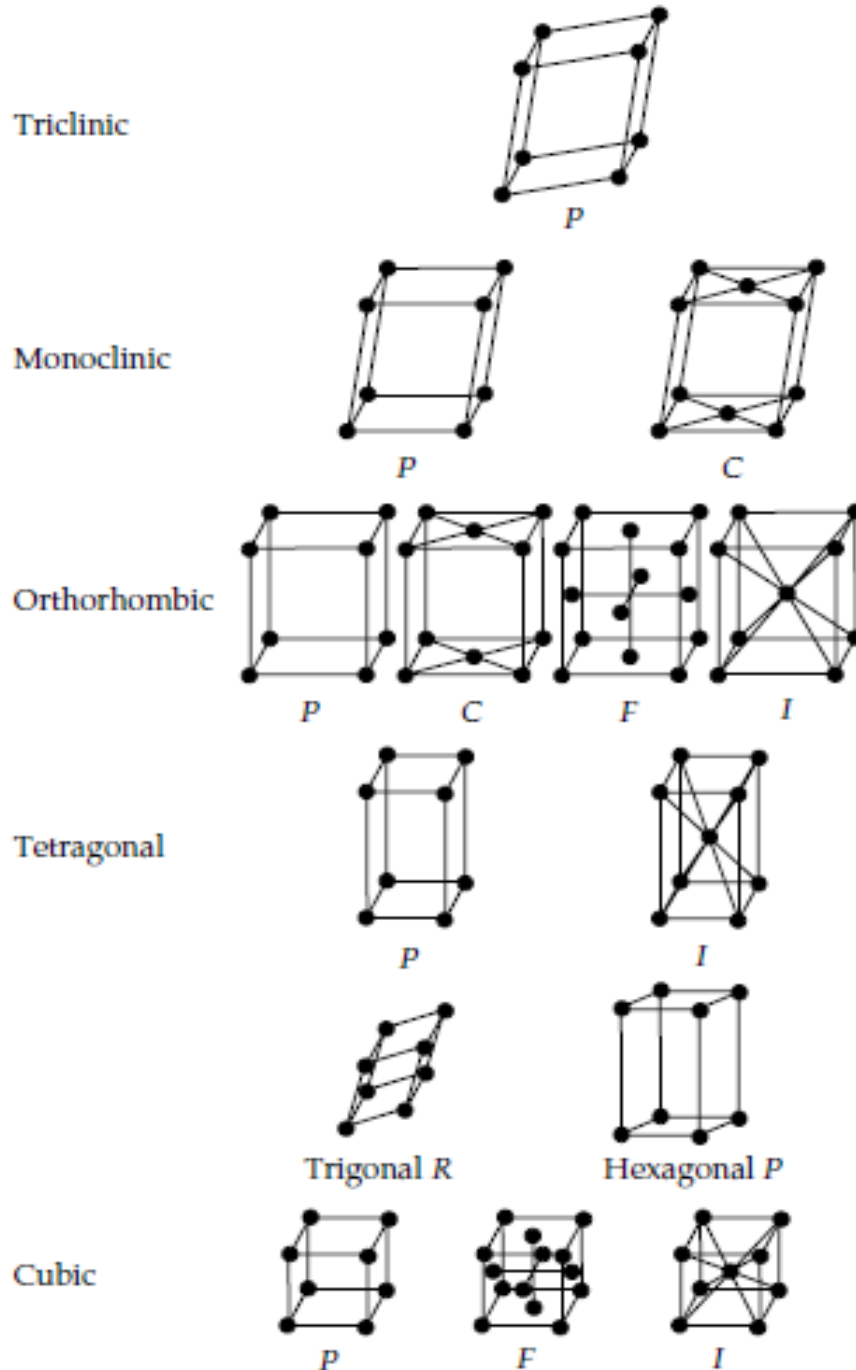

Figure 4.4-2: Bravais lattices [Abd07]

On the other hand, the elements of rotation axes, screw axes, mirror planes, glide planes (no relevant in macromolecule), and inversion centre in a crystal system result

in a crystal symmetry (see Table 4.4-2). Seven crystal systems are existing based on the symmetries. The space group of a crystal is determined by the symmetry elements and centering of cells. There are only 65 space groups related to macromolecules [Abd07]. The details of space groups are listed in Table 4.4-3 [Abd07].

Table 4.4-2: Elements of crystal symmetry [Abd07]

Symmetry element	Description
Rotation axes	Counterclockwise rotation of 360 °/n about an axis, where n is 1, 2, 3, 4, or 6 2-fold axis is rotation by 180 ° 3-fold axis is rotation by 120 ° 4-fold axis is rotation by 90 ° 6-fold axis is rotation by 60 °
Screw axes	Same as rotation axis, but followed by a translation of p/n along the rotation axis, where p is an integer $< n$ 2_1 screw axis is rotation by 180 ° followed by translation of 1/2 of a unit cell 3_1 screw axis is rotation by 120 ° followed by translation of 1/3 of a unit cell 3_2 screw axis is rotation by 120 ° followed by translation of 2/3 of a unit cell 4_1 screw axis is rotation by 90 ° followed by translation of 1/4 of a unit cell 4_2 screw axis is rotation by 90 ° followed by translation of 1/2 of a unit cell 4_3 screw axis is rotation by 90 ° followed by translation of 3/4 of a unit cell 6_1 screw axis is rotation by 60 ° followed by translation of 1/6 of a unit cell 6_2 screw axis is rotation by 60 ° followed by translation of 1/3 of a unit cell 6_3 screw axis is rotation by 60 ° followed by translation of 1/2 of a unit cell 6_4 screw axis is rotation by 60 ° followed by translation of 2/3 of a unit cell 6_5 screw axis is rotation by 60 ° followed by translation of 5/6 of a unit cell
Inversion center	All points inverted through a center of symmetry
Mirror plane	Reflection through a plane
Glide plane	Not relevant in macromolecular crystallography due to the chirality of the biological building blocks

Table 4.4-3: The crystal systems and space groups of macromolecular crystals [Abd07]. Space groups in brackets and parentheses are indistinguishable from diffraction pattern. Those in parentheses are enantiomorphs

Crystal system	Bravais lattices	Restriction on lattice constants	Space group
Triclinic	P	$a{\neq}b{\neq}c$; $\alpha{\neq}\beta{\neq}\gamma$	P1 (no symmetry)
Monoclinic	P, C	$a{\neq}b{\neq}c$; $\alpha{=}\gamma{=}90°$; $\beta{>}90°$	P2, P2$_1$, C2
Orthorhombic	P, C, I, F	$a{\neq}b{\neq}c$; $\alpha{=}\beta{=}\gamma{=}90°$	P222, P222$_1$, P2$_1$2$_1$2, P2$_1$2$_1$2$_1$, C222, C222$_1$, F222, [I222, I2$_1$2$_1$2$_1$]
Tetragonal	P, I	$a{=}b{\neq}c$; $\alpha{=}\beta{=}\gamma{=}90°$	P4, (P4$_1$, P4$_3$), P4$_2$, I4, I4$_1$ P422, (P4$_1$22, P4$_3$22), P4$_2$22, P42$_1$2, (P4$_1$2$_1$2, P4$_3$2$_1$2), P4$_2$2$_1$2, I422, I4$_1$22
Trigonal / rhombohedral	P (or R) [a]	$a{=}b{\neq}c$; $\alpha{=}\beta{=}90°$; $\gamma{=}120°$ $a{=}b{=}c$; $\alpha{=}\beta{=}\gamma{\neq}90°$	P3, (P3$_1$, P3$_2$), R3 [P321, P312], [(P3$_1$21, P3$_2$21), (P3$_1$12, P3$_2$12)], R32
Hexagonal	P	$a{=}b{\neq}c$; $\alpha{=}\beta{=}90°$; $\gamma{=}120°$	P6, (P6$_1$, P6$_5$), (P6$_2$, P6$_4$), P6$_3$ P622, (P6$_1$22, P6$_5$22), (P6$_2$22, P6$_4$22), P6$_3$22
Cubic	P, I, F	$a{=}b{=}c$; $\alpha{=}\beta{=}\gamma{=}90°$	P23, P2$_1$3, F23, [I23, I2$_1$3] P432, (P4$_1$32, P4$_3$32), P4$_2$32, F432, F4$_1$32, I432, I4$_1$32

[a] Rhomobohedral is a subset of the trigonal system in which the unit cell can be chosen on either hexagonal or rhombohedral axes

The key problems which cause the discredit of data integration of single crystal X-ray diffraction are mosaicity and twinning [Rup10]. In the process of crystallization, the foreign ingredients, such as, contaminating proteins, aggregates of denatured protein of interest, will bring multiple crystals. It happens often in practice even though in the process of crystallization by vapor diffusion. In the present work, the single crystals prepared for further crystallography were produced by crystallization

in solution. The growth rate of crystals in solution, in comparison with those in vapor diffusion method, is higher. However, because in the present work it is aim at understanding the crystallization behavior of L-asparaginase II through crystallization in solution (as mentioned in **Chapter 2.5**), the crystals to be identified by X-ray diffraction should be derived from the same environment.
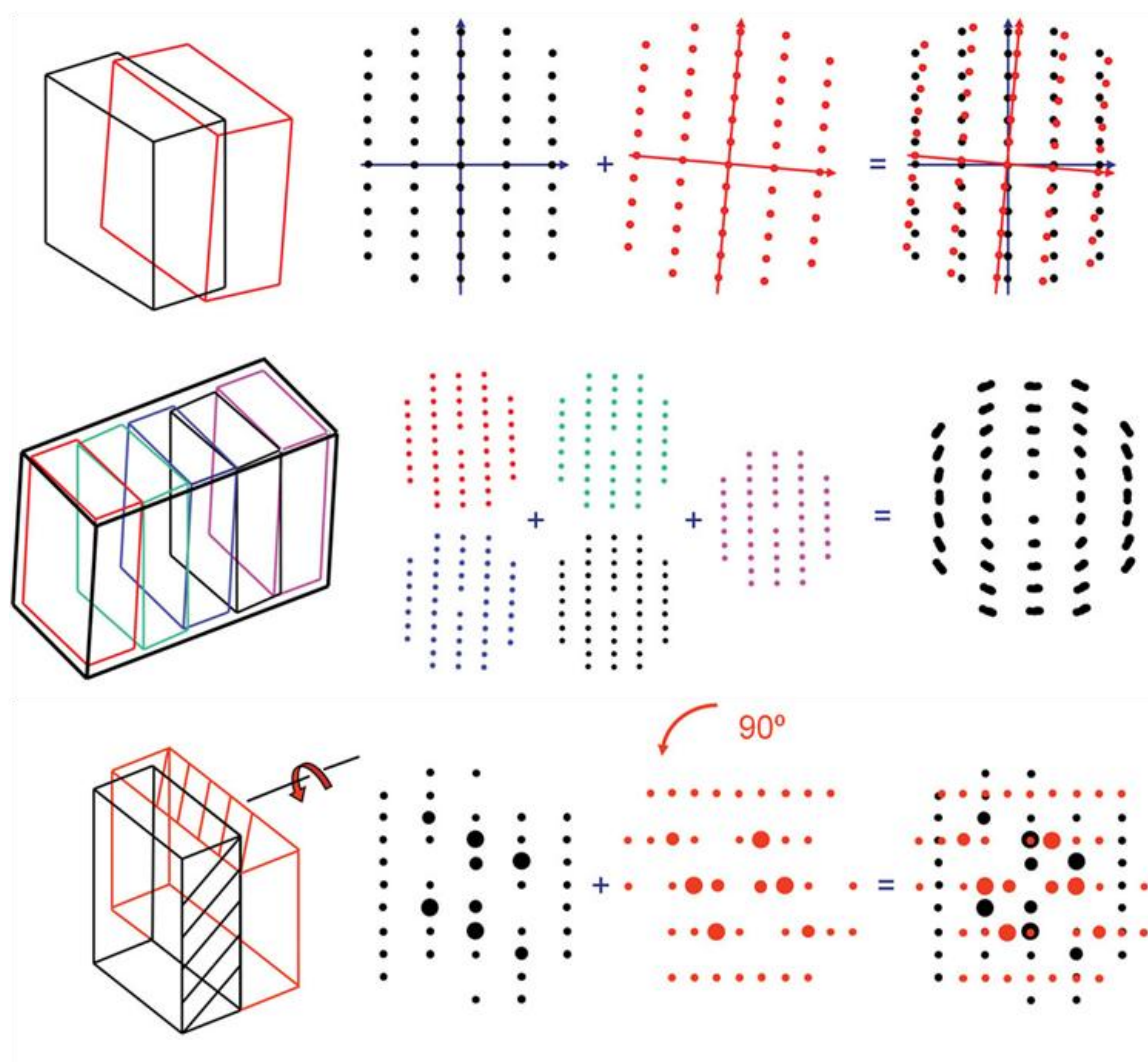
Figure 4.4-3: Diffraction spots result from macroscopic twinning and mosaic crystals [Rup10]

Rupp [Rup10] has summarized that the most common situations, i.e. mosaicity and twinning, is happening on a real imperfect crystal when it is checked by X-ray diffraction. Figure 4.4-3 illustrates the examples of diffraction pattern of a single crystal with mosaicity and twinning [Rup10]. The top example is the diffraction pattern of macroscopic twinning of a crystal. The fact of twinning of a crystal can be

recognized under a microscope. The diffraction pattern of twinning crystals at this condition will overlap but be detached easily from each other. Mostly, a crystal shows perfect quality of appearances, but in fact it consists of many domains inside (see the middle row of Figure 4.5-3). In this case, the crystal is named a mosaic crystal [Rup10]. It seems that the diffraction pattern of this mosaic crystal possesses mosaic spread spots. A third situation in the bottom row of Figure 4.5-3 is that a crystal comprises two domains which match each other just in their two dimensions. This situation is also not visible under a microscope, but the diffraction patterns are penetrated into each other. The diffraction pattern is normally difficult to separate and to be indexed.

In the case of the present work, some single crystals produced by crystallization in solution possess the defects as described in Figure 4.4-3. Figure 4.4-4 illustrates the examples of such defect crystals formed with PEG_{6000} and with ethanol, respectively, achieved in the present work. The flaws on the crystals in Figure 4.4-4 are visible under microscope. Figure 4.4-4a illustrates the crystals formed with PEG_{6000}, and even though the rod-shape crystals have big size in one dimension, there are many small cracks are visible on the surface of the crystals. Figure 4.5-4b illustrates the poor crystals formed with ethanol, which have good sizes in two dimensions, however, they are twinning and mosaic crystals. It can be easily found that the single crystals formed in the presence of ethanol consist of more than one domain. What's more, both crystals (formed with PEG_{6000} and ethanol) have one dimension size far away from the demanding of minimum edge of 0.1mm. Therefore, it could be understood that the diffraction pattern regarding the two kinds of crystals, i.e. formed with PEG_{6000} and ethanol, respectively, are anisotropic.
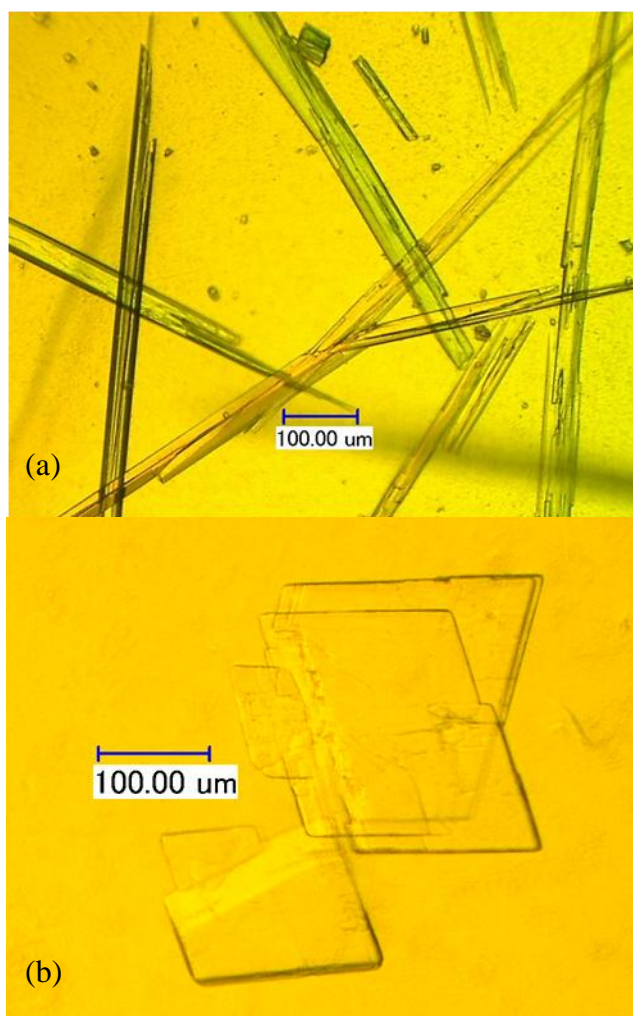
Figure 4.4-4: Big size but poor quality of L-asparaginase II crystals for single crystal X-ray diffraction. (a) crystals formed in the presence of PEG_{6000}; (b) crystals formed in the presence of ethanol

The crystals formed in a given precipitant agent studied in the current work existing differences in their qualities which can be noticed by comparing the growth rates of crystals at different conditions. Table 4.4-4 shows the growth rates of crystalline L-asparaginase II obtained in the present work, and their corresponding microscopic images are illustrated in Figure 4.4-4. Here the average growth rates in Table 4.4-4 were calculated in terms of the volume equivalent radius of a sphere at a constant rate within a given period. The data indicate that the crystals grow faster in the presence of PEG_{6000} (0.23-0.27 $\times$ 10^{-9} m s^{-1}) than those supplemented with ethanol (0.05 $\times$ 10^{-9} m s^{-1}) and with MPD (0.01 $\times$ 10^{-9} m s^{-1}). PEG_{6000} is a polymer and has a different solubility compared to ethanol and MPD, which results in a different growth rate of the crystals and then it attempts to form crystals much faster with PEG_{6000} [Mc09].

The microscopic images of crystals formed with PEG_{6000} in Figures 4.4-5a, b show that the crystals grew extraordinarily fast in one dimension. However, the lower growth rate in the presence of ethanol brings a better geometry of the crystals, which grew in two dimensions at the similar speed (see Figure 4.4-5c). But the crystals grew very slowly in their thickness, especially in the presence of PEG_{6000} and ethanol, even though they were kept in the subsequent two or three months. It is suggested that the size of a single crystal suitable for X-ray diffraction should be at least 0.1 mm in all dimensions [Mye02][Wie02]. In the present work, only the crystals formed with MPD are barely able to fulfill that required dimension (see Table 4.4-1).

Table 4.4-4: Growth rates of crystalline L-asparaginase II formed with a given precipitant agent

Crystals Morphology	Precipitant	Growth Time [h]	Final Size[b] [μm]	Average Growth rate[a] [m s^{-1}]
rod-shape crystals (Figure 4.4-5a)	PEG_{6000}	17	400×23×2	0.27×10^{-9}
rectangle-shape crystals (Figure 4.4-5b)	PEG_{6000}	17	179×34×2	0.23×10^{-9}
rhombus-shape crystals (Figure 4.4-5c)	ethanol	312	246×263×9	0.05×10^{-9}
Prism-shape crystals (Figure 4.4-5d)	MPD	336	57×17×12	0.01×10^{-9}

[a] Here the growth rate is based on the volume equivalent **radius**

[b] Three dimensions size (length×width×thickness)
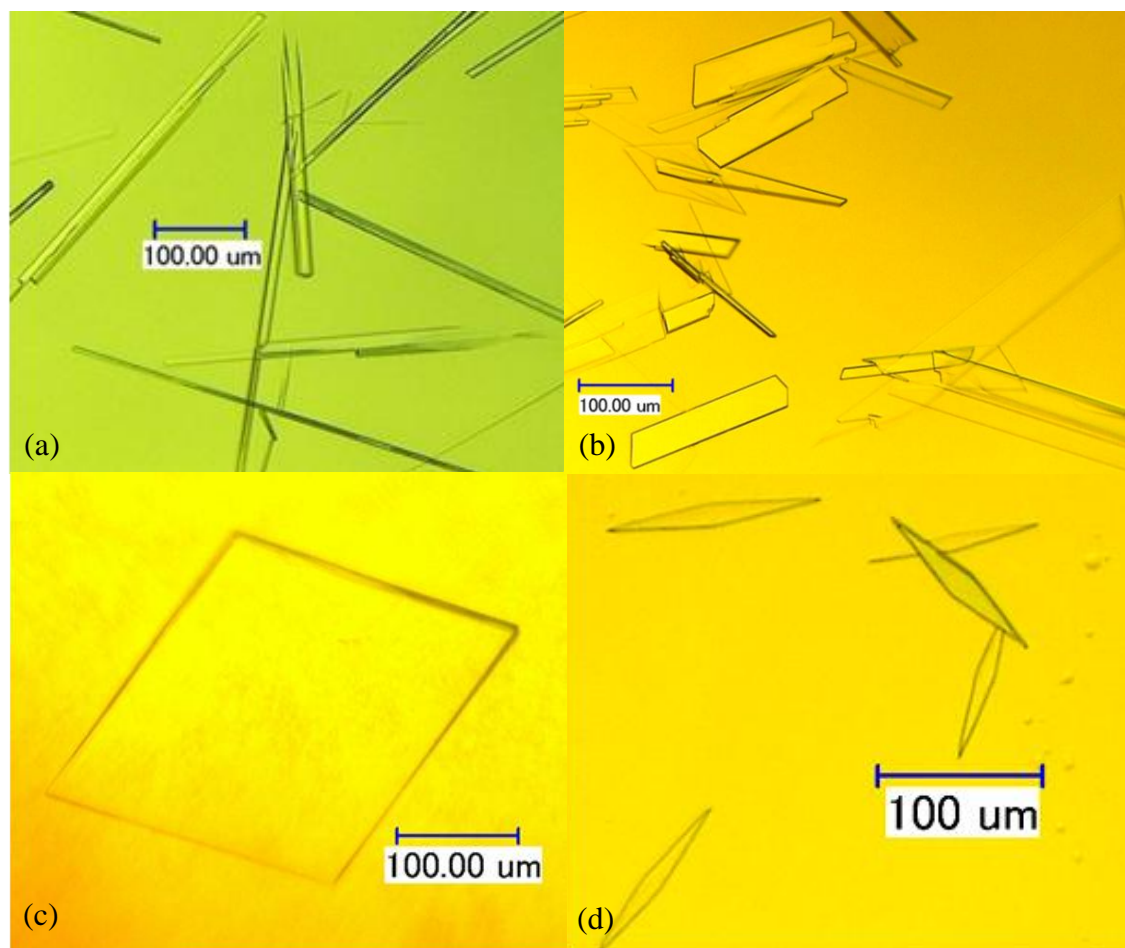
Figure 4.4-5: Microscope images of crystalline L-asparaginase II formed with different precipitant agents observed in a 200 μL microbatch. (a) rod-shape crystals formed with PEG_{6000} in 1st crystallization at 22°C; (b) rectangle-shape crystals formed with PEG_{6000} in recrystallization at 22°C; (c) rhombus-shape crystals formed with ethanol at 8°C; (d) prism-shape crystals formed with MPD at 8°C

As mentioned above, the space group of the single crystal as well as the precipitant agent of MPD was the same as that reported by Palm et al. [Pal96]. it therefore could be assumed that the crystalline structure of L-asparaginase II in this work is similar to that described by Palm et al. [Pal96].

4.4.2 X-ray powder diffraction (XRPD)

Another X-ray method, i.e. X-ray powder diffraction (XRPD), is a common favorite to identify crystals. However, with XRPD it is impossible to determine unknown crystal structures. In comparison with single crystal X-ray diffraction, it is used for chemical analysis and crystals estimation [Mye02]. Nonetheless, XRPD is a good

choice to detect crystals for a comparison, especially if it is impossible to grow a large and perfect single crystal.

Theoretically, the peak positions in an XRPD pattern are related to the crystalline compounds and the crystal symmetry. It is possible to identify a substance when there is a known standard powder diffraction pattern of the corresponding substance. There are 265,127 indexed pattern (37,816 organic) embodied in the database of ICDD (International Centre for Diffraction Data PDF-2). However, there is rarely an exact pattern for a protein structure determination. Von Dreele et al. [Von00] have reported that they were successfully to determine the protein structure of a variant of the T_3R_3 Zn-human insulin complex, by using high-resolution XRPD pattern (the National Synchrotron Light Source). But Von Dreele et al. [Von00] also suggests that this method can be employed to examine structural changes in a series of protein derivatives when the structure of one of these derivatives has been determined by single crystal X-ray diffraction. In the present work, the XRPD pattern is not from high-resolution. Thus, it is impossible to solve and refine both of the crystal structures of L-asparaginase II formed with PEG_{6000} and ethanol, even though there are known structures of L-asparaginase II found in PDB (Protein Data Bank).

The XRPD pattern of crystals obtained by supplementing with ethanol, PEG_{6000} and MPD are presented in Figure 4.4-6, respectively. It is fortunate that the pure PEG_{6000} is a stable powder at room temperature. The crystals structure of L-asparaginase II with respect to a given precipitant agent was analysed by adopting the pure PEG_{6000} powder as a standard reference. Figure 4.4-7 illustrates the differences between the diffraction patterns of pure PEG_{6000} and that of air dried crystals formed in the presence of PEG_{6000}. It is obvious that the typical peaks in the pattern regarding crystals formed with PEG_{6000} are mostly attributed to PEG_{6000} itself. A broad peak existing within the area of $2\theta=7.5\text{-}12.5^{\circ}$ is evident only in the pattern belong to crystals formed with PEG_{6000}. By comparison, in Figure 4.4-6, it is clear that the three pattern of the three crystals all possess such typical broad peak falling within the range of $2\theta=5\text{-}12.5^{\circ}$. The pattern of crystals formed with ethanol (top, red) and those formed with MPD (bottom, green) look identical. They have two typical broad peaks locating at the position of $2\theta=5\text{-}12.5^{\circ}$ and $2\theta=15\text{-}25^{\circ}$. These two broad peaks could be considered as the typical peaks attributing to L-asparaginase II. There are reasons to believe that there is also a broad peak located $2\theta=15\text{-}25^{\circ}$ in the pattern regarding the

dry crystals formed with PEG$_{6000}$, but this broad pattern is just covered by the typical sharp peaks owing to pure PEG$_{6000}$.
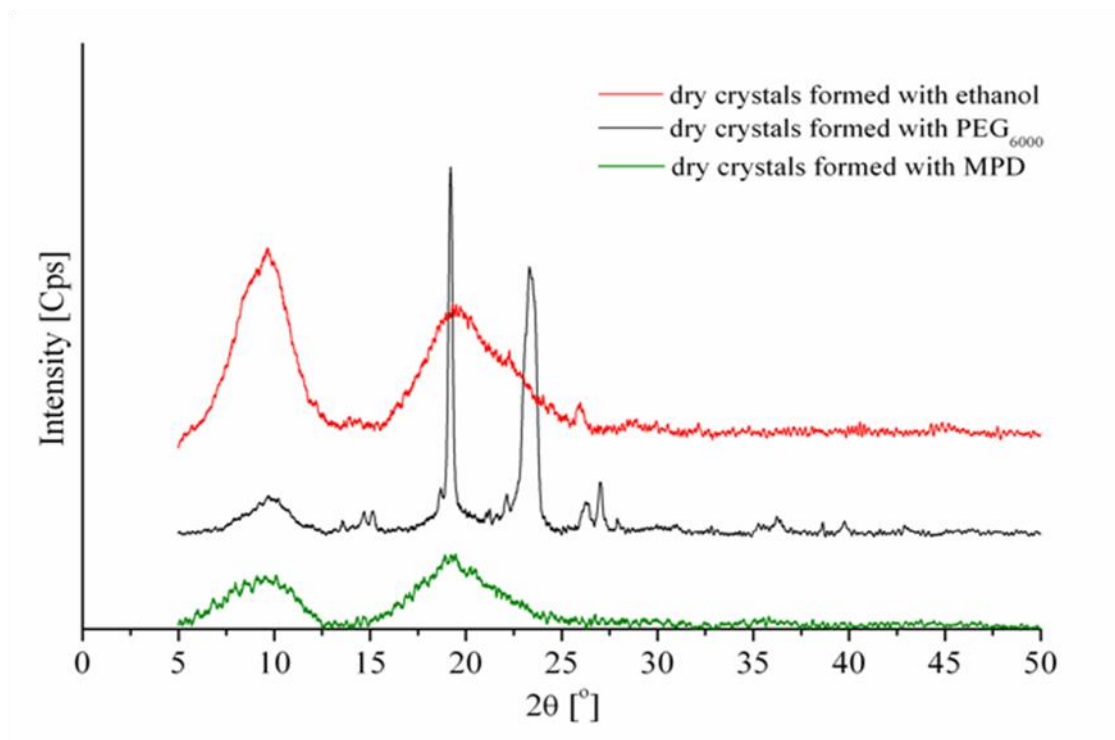
Figure 4.4-6: XRPD patterns of dry crystalline L-asparaginase II formed with ethanol (top), with PEG$_{6000}$ (middle) and with MPD (bottom)
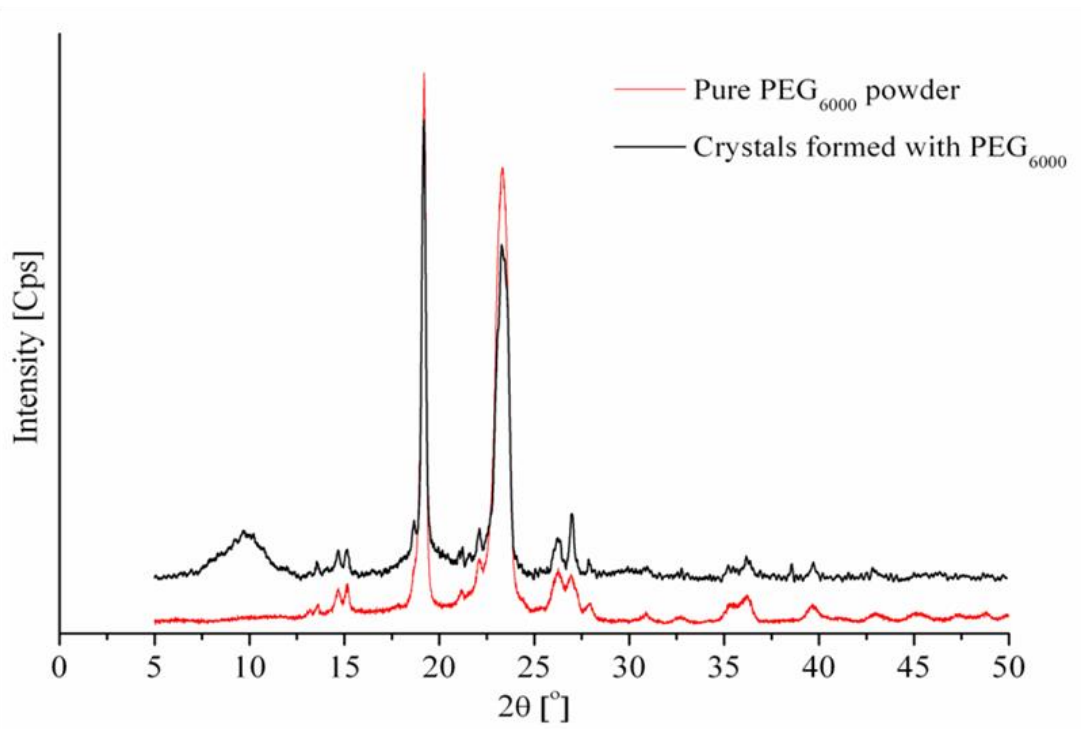
Figure 4.4-7: XRPD patterns of pure PEG$_{6000}$ powder (bottom) and dry crystalline L-asparaginase II formed with PEG$_{6000}$ (top)

Up to date, there is still no XRPD pattern regarding crystalline L-asparaginase II to be found. However, Müller [Mül12] reported the XRPD pattern of lysozyme crystals in her thesis, as shown in Figure 4.4-8. Müller [Mül12] has checked the lysozyme crystlals in three different modifications by XRPD. It is evident in Figure 4.4-8 that the typical sharp peaks in those three patterns are contributed from NaCl. Other two typical broad peaks existing in all three patterns are located in the area of $2\theta=5-10^{o}$ and $2\theta=15-25^{o}$, respectively. A similar phenomenon can be also found in the high-resolution XRPD pattern of T$_3$R$_3$ human insulin-zinc complex reported by Von Dreele et al. [Von00]. Their typical structural peaks in the pattern are also located in the range of $2\theta=1-25^{o}$.
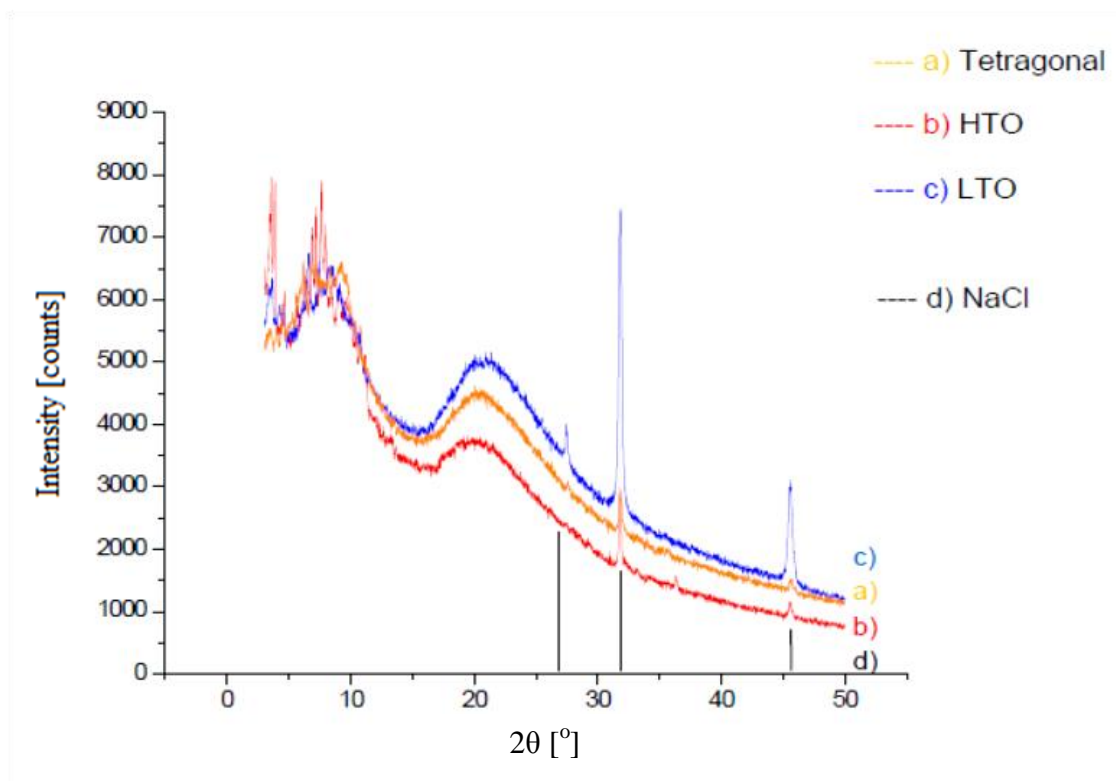
Figure 4.4-8: XRPD pattern of air dried lysozyme crystals [Mül12]

The XRPD results obtained in the present work show that, even though it is impossible by XRPD pattern (without synchrotron) to provide details on a crystal space group, those pattern indicate that the precipitant agent (salts or PEG_{6000}) comprise the internal structure of protein crystals. Of course, in the present work, the XRPD pattern regarding crystals formed with ethanol and MPD have no typical peaks contributed from the precipitant agent, because ethanol and MPD, in comparison with pure PEG_{6000}, are liquid at room temperature. McPherson [Mc99] has declared that macromolecular crystals always consist of 30-90% water, which occupies cavities and channels within the macromolecular crystals. In the case study of lysozyme crystals, Jones, Müller and Ulrich [Jon10][Mül11] had reported that lysozyme crystals contain not only water, but also the buffer solution and precipitant agents in the crystallization media. Therefore, the crystals for a single crystal X-ray diffraction should be fresh separated from their mother liquor, in order to keep their initial complete internal structure. But as to the sample for XRPD measurement, the crystals are normally air dried and are grinded to fine powder. In that case, the water and other liquid components involving in protein crystal structure are removed and then the protein crystals are not integral, especially, when the used precipitant agents are organic

solvent. The protein crystals of T_3R_3 human insulin-zinc complex, whose crystal structure is determined by a high-resolution XRPD reported by Von Dreele et al. [Von00], were obtained in the presence of 1.0 M NaCl. The microcrystalline powder for the XRPD measuring was obtained by grinding the initial crystals with mother liquor. After that, the excess mother liquor was removed, but the powder of crystals was protected against further solvent evaporation [Von00]. Through this process, the integral structure of protein crystals could avoid damage. But it requires a XRPD technique with high-resolution (synchrotron light source) to collect the pattern within the area of $2\theta < 25^o$.

4.5 Conclusion

• L-asparaginase II, extracted from recombinant *Escherichia coli* cells through two times acetone precipitation, was successfully crystallized and thereby purified. A given precipitant agent was used and a simple method of crystallization from solution was applied. PEG_{6000} (a long chain polymer), ethanol (a volatile solvent) and MPD (a low molecular weight polymer and non-volatile solvent) were chosen as the precipitant agents to induce the crystallization in solution.

• The crystallization behavior of L-asparaginase II in the presence of a certain precipitant agent was investigated by an online turbidity technique.

• The classical phase diagram regarding the crystallization of L-asparaginase II was established for the first time, plotting protein concentration versus temperature.

• In order to eliminate the effects of contaminating proteins and inactive protein of interest, new type phase diagram plotting enzymatic activity of L-asparaginase II as a function of temperature was here for first introduced in the present work.

• The space group as well as the unit cell parameters of crystalline L-asparaginase II formed with 26% (v/v) MPD was determined by a single crystal X-ray diffraction. The single crystals suitable for X-ray diffraction were prepared by the crystallization in solution, rather than vapor diffusion technique.

• X-ray Powder Diffraction was applied to identify the structural differences of the crystals obtained in the present work in the qualitative level. The XRPD pattern regarding L-asparaginase II crystals are not found in other works. The XRPD pattern regarding L-asparaginase II crystals are not found in other works up to date.

5. SUMMARY

This work was starting by producing crystalline L-asparaginase II through a simple method of crystallization in solution with a given precipitant agent. Instead of purchasing a commercial product, the L-asparaginase II solution was prepared by a two times acetone precipitation from a recombinant *Escherichia coli* cells. The extract of L-asparaginase II in an initial concentration of 50 mM Tris-acetate buffer pH 5.1 is able to be successfully crystallized by adding a given precipitant, when its specific activity value varies ranging from 26.9 U/mg to 35.7 U/mg.

Further, the crystallization behavior of L-asparaginase II was investigated by an online turbidity technique. The nucleation and solubility data over the range of studied were collected and were plotted in terms of protein concentration versus temperature. In order to eliminate the contaminating proteins and inactive protein of interest, a new type of phase diagram, plotting enzymatic activity as a function of temperature established for the first time. Three types of precipitant agents, i.e., PEG_{6000}, ethanol and MPD, were selected to play the role of precipitant agent for the crystallization. The phase diagrams obtained in the present work were determined falling within the range of 4.1-8.3% (w/v) PEG_{6000}, 13-28.6% (v/v) ethanol, 15.3-22.8 % (v/v) and 28.6% (v/v) MPD, respectively. All curves achieved were "normal", i.e., the solubility of L-asparaginase II crystals increases with an increase of temperature and the spontaneous nucleation occurs at a higher temperature with a higher protein concentration. The phase diagram plotting enzymatic activity versus temperature is from the same type as that plotting protein concentration versus temperature on their upward trend. This result shows that the crystallization behavior over the range of conditions investigated in the present work is contributed from the active L-asparaginase II.

Up to date, the classical phase diagram regarding the crystallization behavior of L-asparaginase II has not been found in other literatures, not to mention the new type phase diagram plotting enzymatic activity versus temperature. The outstanding advantage of introducing the new type phase diagram using enzymatic activity to replace the protein concentration is possible to eliminate the influence of contaminating proteins or inactive protein of interest on the crystallization behavior. It has been especially prominent when the crystallization serves as a purification and separation technology out of a raw material in industrial application.

The nucleation and solubility data regarding the sample solutions supplemented with MPD demonstrate that, the data partly overlap within the MPD concentration of 15.3-22.8% (v/v). But these data would shift to a higher temperature area when the MPD concentration increases to 28.6% (v/v). The same phenomenon in the case study of lysozyme crystals had been reported by Forsythe et al. [For99]. There are reasons to believe that the nucleation and solubility data, collected in the sample solutions supplemented with PEG_{6000} and ethanol, have no big visible change when the PEG_{6000} and ethanol concentrations falling within the range of 4.1-8.3% (w/v) and 13-28.6% (v/v), respectively. But the data will travel an evident distance when PEG_{6000} or ethanol reaches to a higher concentration in the sample solution.

Compared to lysozyme, the MZW achieved in the current work is only up to 11 ℃, which is much smaller than that reported by Maosoongnern el al. [Mao12]. However, the range of conditions investigated in the present work is also smaller than that in the case study of lysozyme. The protein concentration of L-asparaginase II investigated here is no more than 4 mg/mL, while lysozyme with a concentration up to 70 mg/mL was studied by Maosoongnern et al. [Mao12].

Single crystal X-ray diffraction was successfully performed on a crystal prepared in the presence of 26% MPD at 8 ℃ by a simple solution crystallization method. The crystal indicates an orthorhombic form, belonging to the space group of $P2_12_12_1$ with the unit cell parameters a=93.9, b=125.77, c=151.75Å. The crystal diffracted up to a resolution of 2.88Å. It reveals that the method of crystallization in solution is suitable to produce crystals for single crystal X-ray diffraction, if the initial crystal growth rate is smaller than 0.03×10^{-9} m/s (calculated in terms of volume equivalent **diameter**, in 14 days).

The crystals obtained in the present work formed with the three precipitant agents as mentioned above, respectively, were also analyzed by X-ray powder diffraction (XRPD). The pattern regarding the crystals formed with PEG_{6000} represent that the precipitant agent participating in the crystallization will be a component of the crystals structure. The patterns of the three types of crystals show that the typical peaks with respect to the protein structure are located in the small angel area of $2\theta<25°$. The air dried crystals prepared for XRPD analysis will lose their complete structure due to evaporation of the solvent contained in the internal structural of a protein crystal.

The present work made an initial probe to investigate the crystallization behavior of L-asparaginase II, guiding the crystal growth in a multi-component system when the crystallization serves as a technique to purify and separate a protein of interest from a raw material in an industrial application. Further research in this direction is imperative. For the further improvement, it is essential to determine a phase diagram regarding the crystallization behavior of L-asparaginase II over a wider range of conditions. Other kinds of precipitant agent should also be considered in future.

6. ZUSAMMENFASSUNG

Diese Arbeit wurde mit der Herstellung kristalliner L-Asparaginase II durch ein einfaches Verfahren der Kristallisation aus der Lösung mit einem gegebenem Ausfällungsmittel gestartet. Anstatt ein kommerzielles Produkt zu kaufen, wurden die L-Asparaginase II Lösung nach Behandlung der rekombinanten *Escherichia coli* Zellen zweimal mit Aceton ausgefällt. Der L-Asparaginase II Extrakt, der sich in einer Anfangskonzentration von 50 mM Tris-Acetat Puffer pH5.1 gelöst hat, kann durch Hinzufügen eines Ausfällungsmittels kristallisiert werden, wenn seine spezifische Aktivität im Wert zwischen 26,9 U/mg auf 35,7 U/mg variiert.

Weiterhin wurde das Kristallisationsverhalten der L-Asparaginase II durch eine Online Trübungs-Technik untersucht. Die Keimbildungs- und Löslichkeitsdaten wurden über den Bereich der untersuchten gesammelt und wurden hinsichtlich der Proteinkonzentration gegen die Temperatur aufgetragen. Um die verunreinigenden und die inaktiven Proteine, die nicht von Interesse sind, zu beseitigen, wurde ein neuer Typ eines Phasendiagrammes, das die Enzymaktivität der L-Asparaginase II als Funktion der Temperatur zeigt, hier zum erste Mal aufgestellt. Drei Ausfälmitteln, PEG_{6000}, Ethanol und MPD wurden ausgewählt, um die Kristalle zu erhalten. Die Phasendiagramme, die in der vorliegenden Arbeit erhalten wurden, fallen in den Bereich von 4,1 bis 8,3% (w/v) PEG_{6000}, von 13 bis 28,6% (v/v) Ethanol, von 15,3 bis 22,8% (v/v) und 28,6% (v/v) MPD. Alle erzielten Kurven sind "normal", d. h. die Löslichkeit der L-Asparaginase II Kristalle nimmt mit steigender Temperatur zu und mit einer höheren Konzentration des Proteins tritt spontane Keimbildung bei höherer Temperatur auf. Das Phasendiagramm mit der enzymatischen Aktivität als Ordinate und der Temperatur als Abszisse verläuft im Aufwärtstrend gleich, wie die darstellte Proteinkonzentration als Funktion der Temperatur. Dieses Ergebnis bedeutet, dass das Kristallisationsverhalten über einen Bereich von Bedingungen in der vorliegenden Arbeit untersucht wurde, in dem aktive L-Asparaginase II vorliegt.

Bis heute sind die klassischen Phasendiagramme für das Kristallisationsverhalten der L-Asparaginase II nicht in der Literatur zu finden. Das Phasendiagramm darstellt als enzymatische Aktivität gegen der Temperatur ist in diese Form absolut neu! Der herausragende Vorteil der Einführung des neuen Phasendiagrammes durch Enzymaktivität die Proteinkonzentration besteht darin den Einfluss von kontaminierenden Proteinen oder inaktiven Proteins, das nicht für das

Kristallisationsverhalten von Interesse ist, zu eliminieren. Dies ist besonders bedeutlich, wenn die Kristallisation als Reinigungs- oder Trenntechnik aus eines Rohmaterials in der industriellen Anwendung dient.

Die Keimbildungs- und Löslichkeitsdaten der Lösungen unter MPD-Zugabe zeigen, dass sich die Daten in dem interessanten MPD Konzentrationsbereich von 15,3 bis 22,8% (v/v) sich teilweise überlappen. Aber diese Daten verschieben sich zu einem höheren Bereich der Temperatur, wenn sich die MPD Konzentration auf 28,6% (v/v) erhöht. Das gleiche Phänomen existiert in der Fallstudie von Lysozym Kristallen, über das durch Forsythe et al. [For99] berichtet wurde. Es gibt Gründe zu glauben, dass die Keimbildung und die Löslichkeit, die in den Probelösungen mit Zugabe von PEG_{6000} und Ethanol gesammelt wurden, keine große sichtbare Veränderung hervorrufen, wenn PEG_{6000}- bzw. Ethanol-Konzentrationen in den Bereich von 4,1 bis 8,3% (w/v) und von 13,0 bis 28,6% (v/v) fallen. Die Daten werden aber offensichtlich bei einer höheren Temperatur mit einer größeren Zugabe von PEG_{6000} bzw. Ethanol in der Lösung sich verschieben.

Im Vergleich mit Lysozym ist der metastabile Bereich in der vorliegenden Arbeit nur bis zu 11°C breit. Er ist viel kleiner als, der der durch Maosoongnern et al. [Mao12] gefunden wurde. Dies kann daran liegen, dass die Proteinkonzentration der L-Asparaginase II, die hier untersuchten werden, nicht mehr als 4 mg/mL war, aber das Lysozym mit einer Konzentration bis zu 70 mg/mL durch Maosoongnern et al. [Mao12] untersuchten wurde.

Das Einzelkristall X-ray wurde erfolgreich für einen Kristall in der Gegenwart von 26% MPD bei 8°C durch eine einfache Lösung Kristallisationsverfahren erzeuget wurde, durchgeführt. Der Kristall zeigt eine orthorhombische Form, die der Raumgruppe $P2_12_12_1$ mit den Gitterkonstanten a= 93,9, b =125.77, c =151.75Å zugehört. Der Kristall beugte bis zu einer Auflösung von 2.88Å. Es ist offenbar, dass das Verfahren der Kristallisation aus Lösungen geeignet ist, um Kristalle für Einzelkristall X-ray zu erzeugen, wenn die anfängliche Kristallwachstumsgeschwindigkeit kleiner als $0,03 \times 10^{-9}$ m/s (berechnet in Bezug auf das Volumen äquivalenten **Durchmesser**, in 14 Tage) ist.

Die Kristalle, die in der vorliegenden Arbeit mit den drei Fällungsmitteln erhalten wurden, wie oben erwähnt, wurden über Pulver X-ray Diffraktion (XRPD) analysiert. Das Beugungsmuster in Bezug auf die Kristalle mit PEG_{6000} zeigt, dass das Fällungsmittel eine Komponente der Kristallstruktur ist. Die Beugungsmuster der

Kristalle unter Zugabe von unterschiedlichen Fällungsmitteln zeigen, dass die typischen Peaks zu der Proteinstruktur in dem klein Winkelbereich $2\theta < 25°$ liegen. Die in Luft getrockneten Kristalle, die für die XRPD Analyse vorbereitet werden, verlieren ihre komplette Struktur durch Verdampfung des Lösungsmittels, das in der internen Struktur eines Proteinkristalls enthaltene ist.

Die vorliegende Arbeit ist ein Versuch das Kristallisationsverhalten von L-Asparaginase II zu untersuchen. Das Kristallwachstums wird in einem Mehrkomponenten-System durchführt, wenn die Kristallisation als eine Technik dient, um aus einem Ausgangsmaterial über eine industrielle Reinigung und Trennung das Protein von Interesse. Weitere Forschung in diese Richtung ist zwingend erforderlich. Zur weiteren Verbesserung ist es wichtig, ein Phasendiagramm bezüglich des Kristallisationsverhalten von L-Asparaginase II über einen breiteren Bereich von Bedingungen zu bestimmen. Andere Fällungsmittel sollten auch in Zukunft auch berücksichtigt werden.

7. TABLE OF SYMBOLS

Symbol	Meaning	Unit
A	Absorbance	[-]
c	Concentration of clusters with critical nucleus size	[nuclei /mL]
c	Concentration of sample solution (eq. 3.2-1)	[mol/L]
C_s	Geometry of the nucleus	[-]
d	Thickness of the cuvette (eq. 3.2-1)	[cm]
d	The space between the planes in the atomic lattice (eq. 3.2-5)	[nm]
ΔG_{nuc}	Nucleation free energy battier	[J]
I	Intensity of light	[W/m^2]
J_o	Pre-exponential factor	10^{30} [nuclei/cm^3 s]
k	Blotzmann constant	Gas constant per molecule is 1.3805×10^{-23} [J/K]
n	Integer	[-]
S	Relative supersaturation	[-]
T	Temperature	[°C]
U	International unit (enzymatic activity)	[μmol/min]
V_{mol}	Molecular volume	[m^3/mol]
γ	Interfacial energy	[J]
ε	Molar extinction coefficient	[L/mol/cm]
λ	Wavelength of incident wave	[nm]
θ	Angle between the incident ray and the scattering planes	[°]

8. LITERATURES

[Abd07]   Abdel-Meguid, S. S., Jeruzalmi, D., Sanderson, M. R.: First analysis of macromolecular crystals, in: Macromolecular crystallography, eds. Sanderson, M. and Skelly, J., Oxford, New York 2004, 59-75.

[Ald09]   Aldabaibeh, N., Jones, M. J., Myerson, A. S., Ulrich, J.: The solublility of orthorhombic lysozyme crystals obtained at high pH, Cryst. Growth Des. 9 (2009), 3313-3317.

[Ane11]   Anese, M., Quarta, B., Frias, J.: Modelling the effect of asparaginase in reducing acrylamide formation in biscuits, Food Chem. 126 (2011), 435-440.

[Bec00]   Beckmann, W.: Seeding the desired polymorph: background, possibilities, limitations, and case studies, Orga. Proce. Devolop. 4 (2000), 372-383.

[Bec13]   Beckmann, W.: Crystallization, ed. Beckmann, W., Wiley-VCH, Weinheim 2013.

[Bee14]   http://en.wikipedia.org/wiki/Beer-Lambert_law 11.02.2014

[Bon97]   Bonthron, D. T., Jaskólski, M.: Why a "benign" mutation kills enzyme activity. Structure-based analysis of the A176V mutant of saccharomyxes cerevisiae L-asparaginase I, Acta Biochim. Polon. 44 (1997), 491-504.

[Bor01]   Borek, D., Jaskólski, M.: Sequence analysis of enzymes with asparaginase activity, Acta Biochim. Polon. 48 (2001) 4, 893-902.

[Boy71]   Boyd, J. W., Phillips, A. W.: Purification and properties of L-asparaginase from serratia marcescens, J. Bacteriol. 106 (1971) 2, 578-587.

[Bra12]   Bragg, W. L.: The specular reflexion of X-rays. Nature, 90 (1912) 2250, 410-410.

[Bra76]   Bradford, M. M.: A rapid and sensitive method for the quantitation of microgram quantities of protein utilizing the principle of protein-dye binding, Anal.Biochem. 72 (1976), 248-254.

[Cac91]   Cacioppo, E., Munson, S., Pusey, M. L.: Protein solubilities determined by a rapid technique and modification of that technique to a micro-method, Cryst. Growth, 110 (1991), 66-71.

[Cam67]   Campbell, H. A., Maxhburn, L. T., Boyse, E. A., Old, L. J.: Two L-asparaginase from *Escherichia coli* B. Their separation, purification, and antitumor activity, Biochem. 6 (1967) 3, 721-730.

[Car11]   http://www.carlroth.com/catalogue, 07.06.2011

[Ced68]   Cedar, H., Schwartz, J. H.: Localization of the two L-asparaginase in anaerobically grown *Escherichia coli*, J. Biol. Chem. 242(1968), 3753-3755.

[Coo70]   Cooney, D. A., Handschumacher, R. E.: L-asparaginase and L-asparagine metabolism, Annu. Rev. Pharmacol. 10 (1970), 421-440.

[Dep06]   Depmeier, W.: Observation and characterization of structural phase transitions by X-ray powder diffraction, Part. Part. Syst. Charact. 22 (2005), 367-377.

[Die97]   Diederichs, K. Karplus, P. A.: Improved R-factors for diffraction data analysis inmacromolecular crystallography, Nat. Struct. Biol. 4 (1997) 4, 269-275.

[Din08]   Dinnebier, R. E., Billinge, S. J. L.: Principles of powder diffraction, in: Powder Diffraction: Theory and Practice, eds. Dinnebier, R. E. and Billinge, S. J. L., The Royal Society of Chemistry, Cambridge 2008, 1-19.

[Dur96]   Durbin, S. D., Feher, G., Protein crystallization, Annu. Rev. Phys. Chem., 47 (1996), 171-204.

[Ele10]   http://en.wikipedia. org/wiki/electrophoresis. 06.08.2010.

[Enz13]   http://en.wikipedia.org/wiki/Enzyme, 10.09.2013.

[Eva06]   Evans, P.: Scalling and assessment of data quality, Acta Cryst. D62 (2006), 72-82.

[Fis94]   Fischer, E.: Einfluss der Configuration auf die Wirkung der Enzyme, Ber. Dt. Chem. Ges. 27 (1894) 3, 2985–2993.

[For99]   Forsythe, E. L., Judge, R. A., Pusey, M. L.: Tetragonal chicken egg white lysozyme solubility in sodium chloride solutions, J. Chem. Eng. Data, 44 (1999), 637-640.

[Ger08]   Gerber, S., Kirchhof, K., Kressler, J., Schmelzer, C. E. H., Scholz, C., Hertel, T., Pietzsch, M.: Cloning, expression, partial purification and characterization of a designer protein with repetitive sequences, J. Protein Expres. Purif. 59 (2008), 203-214.

[Gil94]   Gilliland, G. L., Tung, M., Blakeslee, D. M., Ladner, J. E.: Biological macromolecule crystallization database, version 3.0: new features, data and the NASA archive for protein crystal growth data, Acta Crystallogr. D50 (1994), 408-413.

[Gra72]   Grabner, R. W., Zimmerman, M., Subjack, W. L., Veber, D. F.: Crystallization of L-asparaginase. United States Patent 3664926, 1972.

[Gru70]   Grundmann, G., Oettgen, H. F.: Experimental and Clinical Effects of L-asparaginase. Springer-Verlag Berlin, Heidelberg 1970.

[Gon11] González-González, M., Mayolo-Deloisa, K., Rito-Palomares, M., Winkler, R.: Colorimetric protein quantification in acqueous two-phase systems, Proce. Biochem. 46 (2011), 413-417.

[Ho69] Ho, P. P. K., Frank, B. H., Burck, P. J.: Crystalline L-asparaginase II from *Escherichia coli* B, Science, 165 (1969), 510-512.

[Ho70] Ho, P. P. K., Milikin, E. B., Bobbitt, J. L., Grinnan, E. L., Burck, P. J., Frank, B. H., Boeck, L. D., Squires, R. W.: Crystalline L-asparaginase from *Escherichia coli* B: I. purification and chemical characterization, J. Biol. Chem. 245 (1970)14, 3708-3710.

[Hof13] Hofmann, G., Melches, C.: Mixing in crystallization processes, in: Crystallization, ed. W. Beckmann, Wiley-VCH, Weinheim 2013, 203-233.

[Jon10] Jones, M., Ulrich, J.: Are different protein crystal modifications polymorphs? a discussion, Chem. Eng. Technol. 33 (2010)10, 1571- 1576.

[Kab10a] Kabsch, W.: XDS. Acta Cryst. D66 (2010), 125-132.

[Kab10b] Kabsch, W.: XDS. Acta Cryst. D66 (2010), 133-144.

[Kar14] http://www.proteinstructures.com/Experimental/Experimental/protein-crystallography.html, 20.02.2014

[Ken58] Kendrew, J. C., Bodo, G., Dintzis, H. M., Parrish, R. G., Wyckoff, H., Phllips, D. C.: A three-dimensional model of the myoglobin molecule obtained by X-ray analysis. Nature, 181(1958) 4610, 662-666.

[Kos58] Koshland, D. E., Application of a theory of enzyme specificity to protein synthesis. Proc. Natl. Acad. Sci. USA, 44 (1958) 2, 98–104.

[Koz02] Kozak, M., Borek, D., Janowski, R., Jaskólski, M.: Crystallization and preliminary crystallographic studies of five crystal forms of Escherichia coli L-asparaginase II (Asp90Glu mutant), Acta Cryst. D58 (2002), 130-132.

[Lae70] Laemmli, U. K.: Cleavage of structural proteins during the assembly of the head of baceriophage T4. Nature 227 (1970) 259, 68-685.

[Lin08] Lin, Y., Zhu, D., Wang, T., Song, J., Zou, Y., Zhang, Y., Lin, S.: An extensive study of protein phase diagram modification: increasing macromolecular crystallizability by temperature screening, Cryst. Growth Des. 8 (2008), 4277-4283.

[Liu10] Liu, Y., Wang, X., Ching, C. B.: Towards further understanding of lysozyme crystallization: phase diagram, protein-protein interaction, nucleation kinetics, and growth kinetics, Cryst. Growth Des. 10 (2010) 2, 548-558.

[Liu13] Liu, Y., Pietzsch, M., Ulrich, J.: Purification of L-asparaginase II by crystallization, Front. Chem. Sci. Eng. 7 (2013) 1, 37-42.

[Mao12] Maosoongnern, S., Borbon, V. D., Flood, A. D., Ulrich, J.: Introducing a fast method to determine the solubility and metastable zone width for proteins: case study lysozyme. Ind. Eng. Chem. Res. 51 (2012), 15251-15257.

[Mar08] Marx, C., Hertel, T., Pietzsch, M.: Purification and activation of a recombinant histidine-tagged pro-transglutaminase after soluble expression in E. *coli* and characterization of the active enzyme, Enzym. Microbi. Technol. 42 (2008), 568-575.

[Mas63] Mashburn, L., Wriston, J.: Tumor inhibitory effect of L-asparaginase, Biochem. Biophysi. Res. Commun. 12 (1963) 1, 50-55.

[Mc99] McPherson, A.: Crystallization of biological macromolecules, Cold Spring Habor, New York 1999.

[Mc04] McPherson, A.: Introduction to protein crystallization, Methods, 34 (2004), 254-265.

[Mc09] McPherson, A.: Crystallization of macromolecules, in: Introduction to macromolecular crystallography, ed. McPherson, A., second edition, Wiley, Hoboken 2009, 19-49.

[Mem12] http://memydr.com/asparaginase/2173, 02.07.2012.

[Mie07] Miers, H. A., Isaac, F.: The spontaneous crystallization of binary mixtures: experiments on salol and betol, Proc. Roy. Soc. Lond. A79 (1907) 531, 322-351.

[Mul01] Mullin, J.W.: Nucleation, in: Crystallization, ed. Mullin, J. W., forth edition, Butterworth-Heinemann, Oxford 2001, 181-214.

[Mül11a] Müller, C., Liu, Y., Migge, A., Pietzsch, M., Ulrich, J.: Recombinant *L*-asparaginase B and its crystallization - what is the nature of protein crystals?,Chem. Eng. Technol. 34 (2011) 4, 571 - 577.

[Mül11b] Müller,C., Ulrich, J.: A more clear insight of the lysozyme crystal composition, Cryst. Res. Technol. 46 (2011), 646 – 650.

[Mül12] Müller, C.: How to describe protein crystals correctly?-case study of lysozyme crystals. PhD Thesis, Martin-Luther-Universität Halle-Wittenberg, Halle, Germany; Shaker Verlag, Aachen 2012.

[Mus97] Muschol, M., Rosenberger, F.: Liquid-liquid phase separation in supersaturated lysozyme solutions and associated precipitate formation/crystallization, Chem. Phys. 107 (1997), 1953-1962.

[Mye02] Myerson, A. S.: Crystals, crystal growth, and nucleation, in: Handbook of Industrial Crystallization, ed. Myerson, A. S., second edition, Butterworth-Heinemann, Boston 2002, 33-65.

[Nak71]   Nakamura, N., Morikawa, Y., Fujio, T., Tanaka, M.: L-asparaginase from E.*coli* Part I. crystallization and properties, Agr. Biol. Chem. 35 (1971) 2, 219-225.

[Nir09]   http://www.nirosoavi.com/high-pressure-homogenization-technology.asp, 04.12.2009.

[Rau70]   Rauenbusch, E., Bauer, K., Kaufmann, W., Wagner, O.: Isolation and crystallization of L-asparaginase from E.*coli*. in: Experimental and clinical effects of L-asparaginase, ed. Grundmann, G., Oettgen, H. F.: Springer-Verlag Berlin, Heidelberg 1970, 31-48.

[Pal96]   Palm, G. J., Lubkowski, J., Derst, C., Schleper, S., Röhm, K., Wlodawer, A.: A covalently bound catalytic intermediate in *Escherichia coli* asparaginase: crystal structure of a Thr-89-Val mutant, FEBS Lett. 390 (1996), 211-216.

[Pol99]   Polikarpov, I., de Oliveira, R. T., Abrahão-Neto, J.: Preparation and preliminary X-ray diffraction studies of a new crystal form of L-asparaginase from *Escherichia coli*, Acta Cryst. D55(1999), 1616-1617.

[Pus88]   Pusey, M. L., Gernert, K.: A mthod for rapid liquid-solid phase solubilitz measurements using the protein lysozyme, Cryst. Growth, 88 (1988), 419-424.

[Rie89]   Ries-Kautt, M. M., Ducruix, A. F.: Relative effectiveness of various ions on the solubility and crystal growth of lysozyme, J. Biol. Chem. 264 (1989) 2, 745-748.

[Rob68]   Robert J, Burson G, Hill J M: New procedures for purification of L-asparaginase with high yield from *Escherichia coli*, J. Bacteriol. 95 (1968) 6, 2117-2123.

[Ros86]   Gosenberger, F.: Inorganic and protein crystal growth- similarities and differences, J. Cryst. Growth, 76 (1986), 618-636.

[Rup10]   Rupp, B.: Instrumentation and data collection, in: Biomolecular crystallography, ed. Rupp, B., Garland Science, New York 2010, 372-436.

[Rye12]   Ryu, B. H., Ulrich, J.: Controlled nucleation and growth of protein crystals by solvent freeze-out, Cryst. Growth Des. 12 (2012), 6126-6133.

[Sch13]   Schmidt, C., Jones, M., Ulrich, J.: The Influence of additives and impurities on crystallization, in: Crystallization, ed. Beckmann, W., WILEY-VCH, Weinheim 2013, 105-127.

[Spe10]   http://en.wikipedia.org/wiki/spectrophotometry, 02.03.2010.

[Ste99]   Stecher, A. L., de Deus, P. M., Polikarpov, I., Abrahão-Neto, J.: Stability of L-asparaginase: an enzyme used in leukemia treatment, Parm. Acta Helv. 74 (1999) 1, 1-9.

[Swa93]   Swan, A. L., Jaskólske, M., Housset, D., Mohana Rao, J. K., Wlodawer, A.: Crystal structure of *Echerichia coli* L-asparaginase, an enzyme used in cancer therapy, Proc. Natl. Acad. Sci. USA, 90 (1993), 1474-1478.

[Ulr06]   Ulrich, J., Jones, M. J.: Heat and mass transfer operations crystallization, in: Unit operations, Encyclopedia of Life Support Systerms (EOLSS), ed. Pohorecki, R., Oxford/UK 2006.

[Von00]   Von Dreele, R. B., Stephens, P. W., Smith, G. D., Blessing R. H.: The first protein crystal structure determined from high-resolution X-ray powder diffraction data: a variant of T_3R_3 human insulin-zinc complex produced by grinding, Acta Cryst. D56 (2000), 1549-1553.

[Wag69]   Wagner, O., Bauer K., Irion, E., Rauenbusch, E., Kaufmann, W., Arens, A.: Ployethylene glycol for fractionation and crystallization of L-asparaginase. Angew. Chem. internat. Edit. 8 (1969) 11, 885-886.

[Wag71]   Wagner, O., Bauer, K., Kaufmann, W., Rauenbusch, E., Arens, A., Irion, E., all of Wuppertal-Elberfeld. United States Patent, 3620926, 1971.

[Wag73]   Wagner, O., Baue,r K., Kaufmann, W., Rauenbusch, E., Arens, A., Irion, E.: Process for the enrichment of L-asparaginase. United States Patent, 3773624, 1973.

[Web08]   Weber, M.: Industrial purification of the enzyme urease from jack beans using crystallization. PhD Thesis, Martin-Luther-Universität Halle-Wittenberg, Halle, Germany; Shaker Verlag, Aachen 2008.

[Whe69]   Whelan, H. A., Wriston, J. C.: Purification and properties of asparaginase from *Escherichia coli* B, Biochem. 8 (1969) 6, 2386-2393.

[Wie02]   Wiencek, J.: Crystallization of proteins, in: Handbook of industrial crystallization, ed. Myerson, A. S., second edition, Butterworth-Heinemann, Boston 2002, 267-285.

[Wil01]   Wilms, B., Hauck, A., Reuss, M., Syldatk, C., Mattes, R. Siemann, M., Altenbuchner, J.: High-cell-density fermentation for production of L-N-Carbamoylase using an expression system based on the *Escherichia coli* rhaBAD promoter, Biotechnol. Bioeng. 73 (2001) 2, 95-103.

Statement of Authorship

I declare that this thesis has been written by myself. The presented content was developed by my own work, unless otherwise acknowledged in the document. It has not been entered in any previous application for a degree. All sources of information have been specifically indicated and acknowledged.

Halle (Saale), 21. 05. 2014   M. Sc. Yi Liu

CURRICULUM VITAE

First Name: Yi

Family Name: Liu

Date of Birth: 21st , September, 1983

Place of Birth: Zhejiang, China

Education Experiences:

September 2003 - June 2007	Zhejiang University of Technology, in China Study: Materials Science and Engineering Final Degree: Bachelor of Engineering
October 2007 – August 2010	Martin Luther University Halle-Wittenberg, in Germany Study: Applied Polymer Science Final Degree: Master of Science
September 2010 – May 2014	PhD at Martin Luther University Halle-Wittenberg, in Germany Center of Engineering, Thermal Process Engineering Degree: Dr. -Ing.

- **Exchange Experiences (October 2012-November 2012):**

Prof. Dr. Piroska Szabó-Révész, Szeged University, Faculty of Pharmacy, Department of Pharmaceutical Technology, 6720 Szeged, Hungary.

Conferences Experiences: PhD position

September 8-10, 2010	BIWIC 17th (Industrial Workshop on Industrial Crystallization): organizer
September 13-16, 2011	ISIC 18th (International Symposium of Industrial Crystallization): poster
June 18-22, 2012	ACHEMA 30th (World Exhibition Congress): presentation
September 7-9, 2012	BIWIC 19th (Industrial Workshop on Industrial Crystallization): presentation

Publications:

[1] Müller, C., Liu, Y., Migge, A., Pietzsch, M., Ulrich, J.: Recombinant L-asparaginase B and its Crystallization-What is the Nature of Protein Crystals? *Chem. Eng. Technol.* 34 (2011) 4, 571-577.

[2] Liu, Y., Pietzsch, M., Ulrich, J.: Purification of L-asparaginase II by Crystallization, *Front. Chem. Sci. Eng.* 7 (2013) 1, 37- 42.

[3] Liu, Y., Pietzsch, M., Ulrich, J.: Determination of the Phase Diagram for the Crystallization of L-asparaginase II by a Turbidity Technique, *Cryst. Res. Technol.* 49 (2014) 4, 262-268.

[4] Liu, Y., Ulrich, J.: Determination of the Phase Diagram for the Crystallization of L-asparaginase II by a Turbidity Technique - part II. -MPD and crystallography studies-, *Cryst. Res. Technol.* 2014, online-published: DOI 10.1002/crat.201400046.